THE RANCH PLAN PLANNED COMMUNITY

PLANNING AREAS 3 AND 4 RUNOFF MANAGEMENT PLAN

Michael Baker INTERNATIONAL

TECHNICAL APPENDIX O.6

Ranch Plan ROMP (2013) Chapter 7

7 Existing Channel Geomorphic Characteristics

7.1 Fluvial Geomorphology Background

The morphology and behavior of channels has long been considered a sensitive indicator of the "state" of any stream as well as a record of processes acting within a watershed. Geomorphic assessments provide broadly applicable principles that govern the response of river channels to change within, or differences between, watersheds. Although it is difficult to predict the precise extent of the change, the nature of change can be estimated. The shape of a channel controls the structure of the flow that travels through it. In addition, a creek adjusts to handle its load and discharge, it is logical to assume that the geometry and size of a channel cross-section are controlled solely by these factors. However, another important control on channel morphology is the nature of bed and bank materials in which a stream establishes itself. In addition, most investigators believe that in these semi-arid regions of California episodic events are generally the governing factor that are primarily responsible for controlling the form and stability of channel systems.

The geomorphic procedures and equations that have been utilized as part of this study are routinely applied throughout the Southwest on similar geomorphic studies. The general engineering study process includes an evaluation that results in a range of answers developed from these procedures. The bracketed range of answers from the procedures will provide general indicators of stability or change since the comparison is for hydraulic stability For example; Maricopa County used these similar procedures on geomorphic studies of similar systems (see *Skunk Creek/Sonora Wash Watercourse Master Plan Report – Lateral Stability Assessment* (JE Fuller, 2001). The channel geometry relationships applied in this study for stable channel geometry were developed for streams that have been stable for long periods of time for specific types of streams. Ephemeral streams are unique and the results are best interpreted as order-of-magnitude estimates of the direction of expected change, rather than the magnitude of future channel adjustments which is the intent of the analysis discussed in the this planning level study.

7.1.1 General Stream Classification – Mainstem San Juan Creek – Central Portion

The channel form of the mainstem central San Juan Creek study reach can be generally categorized as a "**braided channel**" system for the majority of the study area that is confined within incised channel banks, except for some portions that can be classified as a cascade where the channel has been confined and influenced by topographic/geologic features. This classification of the stream type for San Juan Creek is consistent with other detailed geomorphic studies/investigations which also generally defined as a braided channel. Braided channel reaches are characterized by multi-channel forms in which the channels are separated by bars and islands. The characteristics feature of the braided pattern is the repeated division and joining of the channels, and the associated divergence and convergence of flow which contributes to a high rate of fluvial activity. The different physical watershed/stream conditions that are associated with the development of braided channels include: (1) abundant sediment load, (2) erodible banks, (3) highly variable discharge, and (4) steep valley slopes.

7.1.2 Channel Pattern Relationships

Methodology. The slope of a stream has a strong influence on the channel pattern for a given discharge. Numerous researchers have used empirical data, flume studies, and theoretical relationships to establish a threshold slope that separates braided and meandering stream patterns. Four (4) slope-discharge relationships were selected for evaluation of the streams in the study area.

Lane Equations. Lane (1952) published empirical formulas to define the threshold slope for channel pattern, based on data from alluvial sand bed rivers. His equations leave an intermediate zone between the lines defined by the two (2) slope equations where either pattern occurs. The Lane equations for channel pattern are:

$$\mathbf{S_o > 0.010\ Q_m^{-0.25}} \text{ (Braided channels)}$$
$$\mathbf{S_o < 0.001\ Q_m^{-0.25}} \text{ (Meandering channels)}$$

Where S_o = channel slope (ft./ft.), and
Q_m = mean annual discharge (cfs)

The mean annual discharge for the San Juan Creek was estimated from USGS gauge records from the San Juan Creek at La Novia Bridge (Q_m=25cfs).

Leopold & Wolman Equations. The Leopold and Wolman equations (1957) were developed using data from rivers with coarse bed material (D50 > ¼ inch).

$$\mathbf{S_o > 0.06\ Q_{maf}^{-0.44}} \text{ (Braided channels)}$$
$$\mathbf{S_o < 0.06\ Q_{maf}^{-0.44}} \text{ (Meandering channels)}$$

Where S_o = channel slope (ft/ft), and
Q_{maf} = mean annual flood (cfs)

The equations are based on bankfull discharge, which Leopold and Wolman determined to be equal to the mean annual flood. The mean annual flood has a recurrence interval of about 2.33 years. The 2-year discharge was used in this analysis as an approximation of the mean annual flood. Leopold and Wolman found that straight channels could occur on all slopes, and that the occurrence of straight channels had poor correlation to bankfull discharge.

Henderson Equation. Henderson (1961) used Leopold's and Wolman's data, but added a variable describing the mean bed sediment diameter.

S_o > 0.64 D50
1.14 Q_{maf}
-0.44 (Braided channels)

Where S_o = channel slope (ft/ft), and
Q_{maf} = mean annual flood (cfs), and
D_{50} = mean sediment diameter (ft)

Sediment diameter data were obtained from sieve analyses as described in *Section- 12.1.4.1Sediment Grain Size Analysis – San Juan Creek Mainstem*.

Results-San Juan Creek - Application of three (3) channel pattern equations to the study area are shown in the *Table 7-2*. The measured slope for each reach is also shown. Field observations suggest that flow in San Juan Creek is often straight or slightly sinuous and becomes braided at higher flow rates. The channel pattern equations were applied on a reach-by-reach basis. The table compares the predicted channel pattern (braided, intermediate, meandering, single channel, etc.) with the channel pattern observed in the field and on aerial photographs. The predicted channel pattern was indicated by applying the equations described in the previous paragraphs. As shown in the table that follows, the channel pattern equations predict all types of patterns. The conclusion that may be drawn from these variable predictions is that San Juan Creek is in a transitional state with respect to its planimetric form. Therefore, the river pattern may be susceptible to changes in system inputs that affect channel pattern. Also, the pattern for lower flows may tend toward a straight or meandering pattern, while higher discharges will likely result in a more braided channel pattern. The future nature of San Juan Creek is likely to be a compound channel with a straight to meandering single channel low flow inset into a larger braided river channel, which conveys large flood discharges.

The active lower portion of San Juan Creek within the RMV boundary was divided into discrete reaches in order to apply different geomorphic relationships in assessing the river system tendencies and trends. The reaches used for the geomorphic assessment are different than the reaches used in the sediment transport study. The reach designation and the corresponding HEC-RAS river station are provided in the following *Table 7-1.*

Table 7-1: RMV Lower San Juan Creek Geomorphic Assessment Reach Designation

River Reach No.	Downstream HEC-RAS Station	Upstream HEC-RAS Station
1	36074	37186
2	34605	36074
3	33215	34605
4	31649	33215
5	30509	31649
6	28574	30509
7	27176	28574
8	25646	27176

Table 7-2: Lower San Juan Creek - Channel Pattern Relations by Reach

PA-1 CHANNEL PATTERN RELATIONS BY REACH							
REACH	EQUATION	COMPUTED SLOPE* - MEANDER | BRAIDED	OBSERVED SLOPE	EXPECTED PATTERN	OBSERVED PATTERN	Q_M | Q_2 (CFS)	D_{50} (FT)
1	LANE L&W HENDERSON	0.00045 0.00447 0.00374 0.00063	0.00540	BRAIDED BRAIDED BRAIDED	BRAIDED	25 550	0.02625
2	LANE L&W HENDERSON	0.00045 0.00447 0.00374 0.00063	0.00680	BRAIDED BRAIDED BRAIDED	BRAIDED	25 550	0.02625
3	LANE L&W HENDERSON	0.00045 0.00447 0.00369 0.00062	0.00589	BRAIDED BRAIDED BRAIDED	BRAIDED	25 565	0.02625
4	LANE L&W HENDERSON	0.00045 0.00447 0.00369 0.00062	0.00590	BRAIDED BRAIDED BRAIDED	BRAIDED	25 565	0.02625
5	LANE L&W HENDERSON	0.00045 0.00447 0.00369 0.00062	0.00852	BRAIDED BRAIDED BRAIDED	BRAIDED	25 565	0.02625
6	LANE L&W HENDERSON	0.00045 0.00447 0.00369 0.00062	0.00620	BRAIDED BRAIDED BRAIDED	BRAIDED	25 565	0.02625
7	LANE L&W HENDERSON	0.00045 0.00447 0.00366 0.00062	0.01000	BRAIDED BRAIDED BRAIDED	BRAIDED	25 575	0.02625
8	LANE L&W HENDERSON	0.00045 0.00447 0.00366 0.00062	0.00500	BRAIDED BRAIDED BRAIDED	BRAIDED	25 575	0.02625

*: L&W was originally developed for channels with D_{50} > 0.25"
Q2 discharges are Expected Value (EV) exsting conditions

7.1.3 Braided Channel – General Geomorphic Characteristics

An important characteristic of braided rivers is the instability of their channels. Channel abandonment can occur on time scales varying from hours to months and can involve either gradual or sudden changes. The reason for the dynamic nature of braided river channels is rooted in their varying discharge, overall coarse sediment load, and unstable bank materials. During rapidly rising river stage, secondary circulation cells that form within channels quickly increase in intensity. As shown above, divergent flow cells cause the coarsest material being transported to accumulate within the center of the channel. In coarse bedload systems, these accumulations initiate the formation, growth, and downstream migration of channel bars. As a channel bar grows, it deforms or splits the flow, increasing bed shear stresses in channels or chutes on either side of the bar. Because the river is bedload dominated, the bank materials tend to be relatively coarse-grained and erosionally nonresistant. In addition, most braided rivers in California are formed in semiarid settings where little riparian vegetation protects banks. The nonresistant banks of braided rivers allow rapid lateral expansion of channel bars and erosion of the banks as bars grow and propagate downstream. The growth of these bars during floods leads to the establishment of numerous islands that split the channel into multiple individual channels that branch and rejoin frequently.

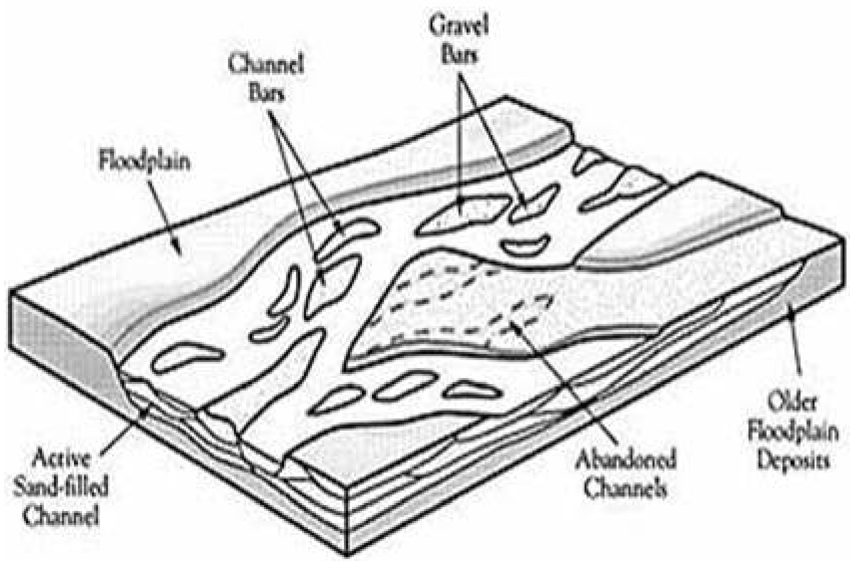

Figure 7-6: General characteristics and definitions of braided channel system

A braided channel is governed by specific conditions of sediment transport competence and capacity relative to sediment transport potential. The particles are within the competence of the watercourse but the supply of sediment exceeds the capacity of the watercourse to move the material. A decrease in sediment supply coupled with an increase in flow energy can destabilize a braided channel system. If there is sufficient coarse-grained material to armor the channel, the braided channel may evolve into a cascade-pool channel form. However, if armoring material is lacking, the channel will destabilize and remain unstable until it erodes down to a more resistant stratigraphic unit or it reduces its slope through planform adjustment. Consequently, the sensitivity of braided channel systems to urbanization depends on maintaining both an adequate supply of sediment to the channel and the physical size of the particles.

Braided channels also tend to have a high width to depth ratio. This means that any increase in flow is spread out over the channel, producing a proportionately small change in stage of flow. Since the forces exerted in the bed are directly proportional to the depth of flow, braided channels exhibit a greater tolerance to alterations in the sediment-flow regime when compared to meander-pool-riffle morphologies. However, water flows tend to focus where the channel finds a weaker bed material and down-cutting ensues. The morphology will change to a single thread channel and down-cutting accelerates.

Individual channel in a braided system are seldom in equilibrium and may be very unstable. As a result the braided channel pattern has been regarded as disequilibrium, aggradational response to an increased sediment load which the stream cannot totally transport. However, many consider that braiding can be a valid equilibrium form given the right combination of discharge and slope, even though the individual channels might be transient. Leopold and Wolman (1957) argued that braiding is the type of adjustment made by streams with erodible banks and a debris load too large to be carried by a single channel, representing a single combination of the adjustable variables which, once established, can be maintained with only slight modification. Some of the key geomorphic characteristics of a braided system are summarized in the following table which is representative of the *stream classification system* suggested by Montgomery and Buffington (1993).

Braided Stream Characteristics
Typical Bed Movement: Variable
Bedform Pattern: Laterally/oscillary
Reach Type: Response
Dominant Roughness Elements: Bedforms (bars, pools)
Dominant Sediment Sources: Fluvial bank failure, debris flows
Sediment Storage Elements – Overbank, bedforms
Typical Slope: S<0.03
Typical Confinement: Unconfined
Pool Spacing (Channel Widths): Variable

7.2 Longitudinal Creek Profile Trends

The longitudinal profile is a plot or picture of the variation in the elevation of the channel along the stream. The following *Figure 7-7* illustrates the longitudinal profile of the San Juan Creek over the study reach from downstream of the Ortega Highway Bridge to just downstream of the confluence with Chiquita Canyon. The data reflect the minimum elevation in the channel as defined in the HECRAS model created by PACE for the purposes of the baseline floodplain mapping. A regional profile extending beyond the study limits has also been provided in the subsequent exhibits of this section which illustrates the regional trends for the river system.

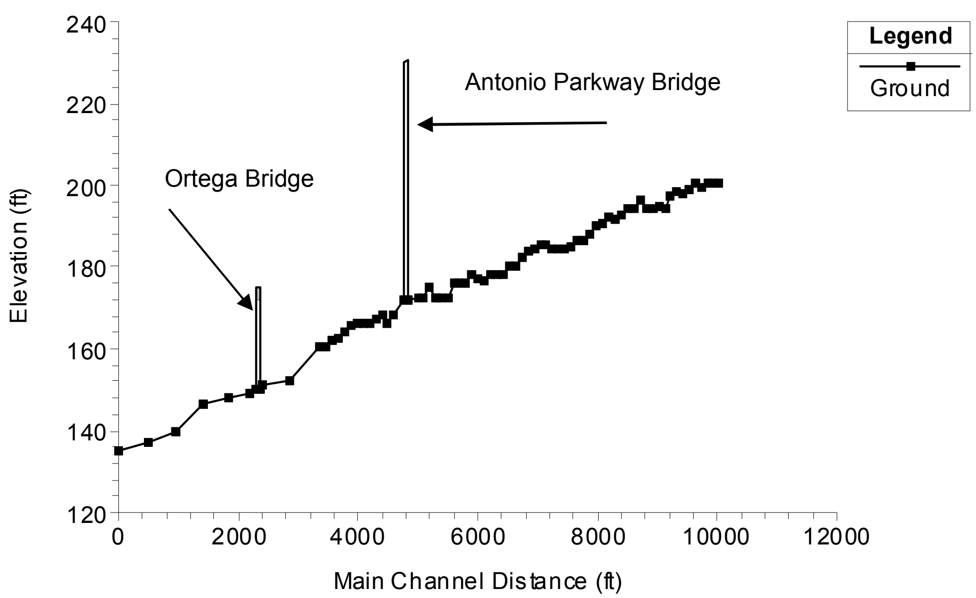

Figure 7-7: Profile of existing mainstem San Juan Creek stream profile within RMV based on digital topography in HEC-RAS cross sections

Graded streams, that is, streams that have adjusted themselves to the prevailing conditions of sediment and water discharges over a long period of time, tend to exhibit smooth concave up longitudinal profiles. The San Juan Creek profile in the study reach is slightly concave up. This shape is more noticeable if one turns the page and looks 'up' the profile from the downstream end. This general regional concave pattern for the San Juan suggests that perhaps San Juan Creek has been a reasonably graded braided river over a long period of time. Although often associated with 'over-loaded' aggrading streams, a braided channel pattern can be considered an equilibrium condition. The following other noteworthy characteristics with respect to the longitudinal profile of the river can be developed.

7.3 Historic Trends/Movement – San Juan Creek Mainstem

The following discussion of the sequence of historical aerial photographs provides a qualitative overview of the physical changes that have occurred on the San Juan Creek during the period of record. The discussion focuses on the character o the river channel in both planimetric form and relative width, as well as on the encroachment of residential developments and agricultural operations into the floodplains and main channel of the river. Historical aerial photographs for each of the years of coverage for the study area are provided in the report. Not all of the years of coverage are available for every part of the study reach. Historical Photo Sequence: 1930, 1938, 1986, and 2005. In the study reach, the overall channel has remained consistent through the period of record. Only in the 2005 aerial does Antonio Parkway cross the channel. There has been significant agricultural development from 1938 to 1986. The 2005 aerial shows further agricultural development as well as roadway development west of Antonio Parkway. Vegetation seems to have thickened in the later photos (1986, 2006).

Measurements of historical lateral channel movement were made from aerial photographs of the study reach. Width changes occur when the channel position remains essentially unchanged, but the channel becomes wider or narrower. Width changes can occur in response to floods, droughts, encroachment, channelization, or changing watershed conditions. Changes in channel position were considered over the entire study reach by comparing the thalweg position shown in aerial photographs. Channel position can change over time due to bank erosion or avulsions during periods of flow, narrowing due to incision or floodplain accretion, or physical relocation of the channel to accommodate human activities. Long-term lateral movement was analyzed by analyzing changes in channel width and by comparing changes in thalweg position over the period of record of the historical aerial photographs.

7.3.1 Channel Width

Channel width is defined as the distance between the channel banks. For San Juan Creek, application of this definition of width requires some judgment for several reasons. First, San Juan Creek is braided, meaning that there is typically more than one (1) channel, and therefore, more than one (1) set of banks. If the width of only one (1) of the braids is measured, then the width is underestimated. If the width between the outermost banks is measured, then areas between braids that are not truly part of the channel are included and the channel width is overestimated. Second, because San Juan Creek is subject to channel change, avulsions, long-term degradation, and human interference, there may be no temporal continuity between the dates of the aerial photographs. That is, a channel visible in one (1) photograph may no longer exist in the next photograph, or an entirely new channel may be formed in another part of the floodplain. Therefore, direct comparison of widths is difficult. Third, in reaches where low floodplains are present, the visible differences between the channel and floodplain are subtle, which makes identifying the banks difficult. Fourth, if the Creek becomes incised, the abandoned former channel often remains visible and may have more readily identified bank characteristics than the current, active channel. Finally, San Juan Creek has a compound channel. That is, the low flow channel(s) exist within a larger flood channel, which may also exist within a higher flow channel, all of which have channel characteristics and banks. Therefore, there are multiple widths to be considered, making comparisons between time periods difficult.

7.3.2 Historical Channel and Bank Positions

Channel thalweg and primary bank positions were digitized and compared from the aerial photographs. The plots of thalweg position shows that the channel thalweg has moved back and forth during the past 75 years. In 1986, the thalweg seems to be at its widest through the period of record. Agricultural development exists along the banks surrounding Antonio Parkway in the later years (1986, 2005). Dense vegetation lines the south bank for all years and along the north bank in the later years (1986, 2005).

7.3.3 Longitudinal Profiles

The interpretation and comparison of longitudinal profiles reveals changes in channel slope or stream bed elevation that may have occurred along the Creek. Changes in the channel slope may indicate adjustments to hydrologic changes or human activity. Degradation or aggradation of the channel bed can also be determined from the comparison of longitudinal profiles.

In a previous study prepared by SLA, multiples years and sources of elevations are compared. However, in the study reach, only the 1970 COE and the 1964 thalweg elevations are available. Near Antonio Parkway, there is up to a 10 feet difference in the elevations for the two (2) years. However, upstream of Antonio Parkway, surrounding the Chiquita Canyon confluence, the change in elevation is less extreme, approximately 3 to 6 feet. Previous studies by Jaffe (in press) suggest that thalweg elevation is only on indication of overall bed elevation at a given cross section. Generally, changes in thalweg elevation are greater than changes to entire sections.

7.3.4 Summary of Historical Variation – San Juan Creek

The historical creek geometry variation was analyzed based on the 1930, 1938, 1986, and 2005 aerial photographs. These photographs show that the channel shape has remained consistent throughout the period of record. There has been some lateral movement in the channel at the upstream and downstream ends of the study reach, where the channel has also narrowed significantly. Analysis of the channel width show a 40% decrease in channel area for the study reach from 1930 to 2005. However, the more significant change in channel area occurs after 1986. Agricultural development has occurred notably surrounding Antonio Parkway in the 1986 and 2005 aerials. In the 2005 aerial, it can also be seen that Antonio Parkway was extended in the northern direction, crossing the channel where it had not before. Analysis of the channel thalweg shows lateral movement in each photograph. In 1986, the thalweg seems to be at its widest in the period of record. Vegetation also seems to be thicker in the later years (1986, 2005). Based on a profile from a previous study prepared by SLA, there appears to be up to a 10 feet difference between the 1970 COE and the 1964 thalweg elevations near Antonio Parkway. However, upstream of Antonio Parkway, surrounding the Chiquita Canyon confluence, the change in elevation is less extreme, ranging approximately from 3 to 6 feet.

7.4 Geomorphic Methods

Regime equations and hydraulic geometry analyses attempt to relate measurable stream characteristics, such as sediment size, mean annual discharge or bankfull discharge, to equilibrium channel geometry characteristics such as stream width, channel depth, flow velocity or channel slope. Regime theory originated from studies of non-scouring and non-silting stable alluvial canals (cf., Kennedy, 1895), and has been extended to a wide variety of stream types (cf., Ackers & Charlton, 1971; Blench, 1951). Regime equations are typically based on discharge, sediment characteristics, and channel geometry. Hydraulic geometry analyses are theoretically similar to regime theory, but are based on empirical data gathered from natural streams or flumes and are typically based solely on discharge. Hydraulic geometry expresses the variation of channel characteristics with increasing discharge at a single section or along the length of a stream. The U.S. Geological Survey (cf., Leopold & Maddock, 1953) published the most widely used hydraulic geometry data.

Regime equation and hydraulic geometry analyses were applied to the ROMP analyses of the study creeks reaches to evaluate the following stream characteristics:

- Channel pattern
- Channel geometry
- Hydraulic geometry

Channel geomorphic trends and stability was evaluated by comparing predicted stream characteristics from one (1) or more of these methodologies to the observed characteristics. These analyses assume that over the long-term the alluvial rivers will tend to erode their bed and banks, or adjust their slope or channel pattern to better match the expected characteristics. In addition, even though regime equations and hydraulic geometry relationships are empirically derived using data sets from very specific stream types (e.g., sand-bed rivers, canals, etc.), the data typically still have a large amount of scatter. The scatter in the original data limits the accuracy of the results. To increase the accuracy of the results, the equations selected for this study were based on data sets from streams which were the most similar to the study area characteristics. It is noted that ephemeral streams in central Arizona are unique, and therefore the results obtained by applying these equations must be interpreted cautiously. In general, the results are best interpreted as order-of-magnitude estimates of the direction of expected change, rather than precise predictions of the magnitude of future channel adjustments.

7.5 Channel Geometry Relationships

Methodology- Equations for stable channel geometry have been developed from streams that have been stable for long periods of time. These equations relate bankfull channel width, depth, and velocity to a specific discharge rate, such as the average annual flow or the dominant discharge. Several stable geometry equations were applied to San Juan Creek to assess the expected direction of future channel change.

Bray Equation #1. Bray (1979) developed equations for the geometry of alluvial gravel-bed rivers based on the 2-year discharge

$$\mathbf{W = 2.38\ Q_2^{\ 0.527}}$$
$$\mathbf{d = 0.266\ Q_2^{\ 0.33}}$$
$$\mathbf{V_m = 8.0\ d^{0.6}\ S_o^{\ 0.29}}$$

Where W = surface flow width (ft)
Q_2 = 2-year discharge (cfs)
d = flow depth (ft)
V_m = mean channel velocity (ft/sec)
S_o = channel slope (ft/ft)

Bray Equation #2. Bray later modified his channel geometry relationships (Hey et. al., 1982) for gravel-bed rivers to include bankfull discharge and the bed material size.

$$\mathbf{W = 2.08\ Q_{bf}^{\ 0.528}\ D_{50}^{\ -0.07}}$$
$$\mathbf{d = 0.256\ Q_{bf}^{\ 0.331}\ D_{50}^{\ -0.025}}$$
$$\mathbf{V_m = 1.87\ Q_{bf}^{\ 0.14}\ D_{50}^{\ 0.095}}$$
$$\mathbf{So = 0.0965\ Q_{bf}^{\ -0.334}\ D_{50}^{\ 0.586}}$$

Where W = surface flow width (ft.)
Q_{bf} = Bankfull discharge (cfs)
D_{50} = medium bed sediment diameter (ft)
d = flow depth (ft)
V_m = mean channel velocity (ft/sec)
S_o = channel slope (ft/ft)

Hey Equation. Hey (1982) developed regime equations for gravel bed rivers in England that relate stable channel geometry to bankfull discharge and bedload transport rate.

$$\mathbf{WP = 2.2\ Q_{bf}^{\ -0.54}\ D_{50}^{\ -0.05}}$$
$$\mathbf{R = 0.161\ Q_{bf}^{\ 0.41}\ D_{50}^{\ -0.15}}$$
$$\mathbf{d_{max} = 0.252\ Q_{bf}^{\ 0.38}\ D_{50}^{\ -0.16}}$$
$$\mathbf{S_o = 0.679\ Q_{bf}^{\ -0.53}\ Q_s^{\ -0.13}\ D_{50}^{\ 0.97}}$$

Where WP = Wetted perimeter (m)
Q_{bf} = Bankfull discharge (m)
D_{50} = Median sediment diameter (m)

R = Hydraulic radius (m)
d_{max} = Maximum channel depth (m)
S_o = Channel slope (m/m)
Q_s = Bedload sediment discharge (%)

Ackers & Charlton Equation.1 The Ackers and Charlton (1971) equations were based on data from flume studies which used sand bed materials.

$$\mathbf{W = K_{ac}\ Q^{0.42}}$$

Where W = surface channel width (ft)
Q = discharge (cfs)
K_{ac} = a coefficient varying from 3.6 for straight channels to 7.2 for meandering channels

Lacey Equation. The Lacey equation (1929) was developed to describe the geometry of siltladen canals in India. However, Bray reported (1979) that in gravel rivers in Canada, the Lacey equation was as accurate for predicting velocity as the Manning's equation.

$$\mathbf{V = 0.8Q^{0.167}}$$

Where V = mean channel velocity (ft/sec)
Q = discharge (cfs)

Chang Equation. Chang's (1988) gravel bed equations for channel geometry support the FLUVIAL-12 sediment transport model, which attempts to simulate channel change from sediment continuity data using minimum stream power concepts. Chang provides equations for channel width, depth, and slope.

$$\mathbf{S_o = 0.000442\ D_{50}\ 1.15\ /\ Q_b^{0.42}}$$
$$\mathbf{W = [1.905 + .249(ln(0.001065\ D_{50}^{1.15}\ /\ (S_o\ Q_{bf}042))2]\ Q_{bf}^{0.47}}$$
$$\mathbf{d = [0.2077 + 0.0418(ln(0.000442\ D_{50}\ /\ (S_o\ Q_{bf}0.42)))1.151\ Q_{bf}^{0.42}}$$

Where S_o = channel slope (ft/ft)
D_{50} = median sediment diameter (mm)
Q_{bf} = bankfull discharge (cfs)
W = channel width (ft)
d = average channel depth (ft)

Some of the predicted channel geometry values were well outside the range of possibility (e.g., negative flow depths). Therefore, the results of the Chang equation are included in the Table, but the predicted values were not used to obtain the average predicted values that were compared with existing reach characteristics.

Kellerhalls (1967) Equations. Kellerhals developed equations for the equilibrium channel width and depth in gravel bed rivers. The Kellerhals equations use the dominant discharge, which is also referred to as the channel-forming or effective discharge.

$$\mathbf{W = 1.8\ Q_{dd}^{.5}}$$
$$\mathbf{d = 0.166\ Q_{dd}0.4\ K_n^{-0.12}}$$

Where W = channel width (ft)
Q_{dd} = dominant discharge (cfs)
d = average channel depth (ft)
K_n = Nikuradse's sand grain roughness coefficient

Here, it is assumed that K_n is twice the mean sediment diameter.

AMAFCA Equations. The AMAFCA (1994) equations for width and equilibrium slope were developed from empirical and theoretical data for application to the arroyo systems of northern New Mexico.

$$\mathbf{W = 0.5\, F^{0.6}\, Fr^{-0.4}\, Q^{0.4}}$$
$$\mathbf{S_o = 18.28\, n^2\, F^{0.133}\, Fr^{2.133}\, Q^{-0.133}}$$

Where W = width of channel (ft)
F = width/depth ratio
Fr = main channel Froude number
Q = discharge (cfs)
S_o = channel slope (ft/ft)
n = Manning's 'n' value for channel

Moody & Odem Equations. Moody and Odem (1999) recently completed an investigation of bankfull channel geometry relationships on a variety of stream types in Arizona using Rosgen channel classification methods.

$$\mathbf{Q_{bf} = 52.334\, DA^{0.5766}}$$
$$\mathbf{A = 11.428\, DA^{0.5291}}$$
$$\mathbf{TW = 12.301\, DA^{0.3756}}$$
$$\mathbf{d = 0.9455\, DA^{0.1506}}$$

Where Q_{bf} = Bankfull discharge (cfs)
DA = Watershed drainage area (mi^2)
A = Section flow area at bankfull discharge (ft)
TW = Flow width at bankfull discharge (ft)
d = Average flow depth at bankfull discharge (ft)

Results – San Juan Creek - The results of applying the channel geometry equations to San Juan Creek are shown in *Table 7-3*, below. The 2, 10, and 100-year discharges were substituted for the discharge variable used in the original channel geometry equations to examine the trend of potential adjustments in channel geometry at each flow rate. Predicted values of widths, depths, slopes and velocities from the channel geometry equations were compared to the measured values obtained from field data, topographic mapping and HEC-RAS models. The differences were interpreted as follows:

- Width. Where the predicted channel width is greater than the HEC-RAS modeled channel width, the channel is expected to erode its banks to achieve the greater width during future floods. Where the predicted channel width is less than the HEC-RAS modeled channel width, the channel is assumed to have low potential for lateral movement due to channel widening, and is likely to experience deposition along the banks, at least at the flow rates considered.
- Depth. Where the predicted channel depth is greater than the HEC-RAS modeled channel depth, the channel is expected to erode its bed (degrade) to achieve the equilibrium depth during future floods. Where predicted channel depth is less than the HEC-RAS modeled channel depth, the channel is expected to aggrade (deposit sediment) to reach the equilibrium state.
- Slope. Where the predicted slope is less than the existing slope, the channel is expected to decrease its slope (scour) to achieve a more stable form.
- Velocity. Where the predicted velocity is less than the HEC-RAS modeled velocity, floods will be more erosive than predicted by the channel geometry equations.

Table 7-3: Lower San Juan Creek - Channel Geometry Relationship Analyses

LOWER SAN JUAN CREEK REACH 1 CHANNEL GEOMETRY REALTIONS												
EQUATION / PARAMETER	CHANNEL WIDTH (FT)			FLOW DEPTH (FT)			SLOPE (FT/FT)			VELOCITY (FPS)		
	Q_{100}	Q_{10}	Q_2	Q_{100}	Q_{10}	Q_2	Q_{100}	Q_{10}	Q_2	Q_{100}	Q_{10}	Q_2
BRAY - 1	544.5	233.2	13.0	8.0	4.7	0.8	-	-	-	-	-	-
BRAY - 2	620.4	265.2	14.7	8.5	5.0	0.8	0.00037	0.00063	0.00390	5.6	4.5	2.1
HEY	-	-	-	7.1	3.8	0.5	0.00022	0.00052	0.00949	-	-	-
A&C / LACEY*	410.0	208.6	20.9	-	-	-	-	-	-	4.5	3.4	1.4
CHANG	1198.7	458.8	15.8	-6.5	-2.2	0.1	0.00051	0.00026	0.00003	-	-	-
KELLERHALS	311.8	139.4	9.0	14.6	7.7	0.9	-	-	-	-	-	-
AMAFCA	347.0	214.5	28.7	-	-	-	0.00754	0.00556	0.00990	-	-	-
M&O	-	-	65.6	-	-	1.9	-	-	-	-	-	5.7
AVERAGE	572.1	253.3	24.0	9.5	5.3	1.0	0.00216	0.00174	0.00583	5.0	3.9	3.0
HEC-RAS	499.3	264.7	230.3	10.7	5.1	3.4	0.00643	0.00595	0.00610	10.4	6.4	4.7
BANKFULL	-	-	230.3	-	-	3.4	-	-	0.00610	-	-	4.7
EXPECTED BEHAVIOR	DEG	AGG	AGG	AGG	DEG	AGG	DEG	DEG	DEG	DEG	DEG	DEG

LOWER SAN JUAN CREEK REACH 2 CHANNEL GEOMETRY REALTIONS												
EQUATION / PARAMETER	CHANNEL WIDTH (FT)			FLOW DEPTH (FT)			SLOPE (FT/FT)			VELOCITY (FPS)		
	Q_{100}	Q_{10}	Q_2	Q_{100}	Q_{10}	Q_2	Q_{100}	Q_{10}	Q_2	Q_{100}	Q_{10}	Q_2
BRAY - 1	544.5	233.2	13.0	8.0	4.7	0.8	-	-	-	-	-	-
BRAY - 2	620.4	265.2	14.7	8.5	5.0	0.8	0.00037	0.00063	0.00390	5.6	4.5	2.1
HEY	-	-	-	7.1	3.8	0.5	0.00022	0.00052	0.00949	-	-	-
A&C / LACEY*	410.0	208.6	20.9	-	-	-	-	-	-	4.5	3.4	1.4
CHANG	3195.5	1312.2	59.0	-19.7	-8.9	-0.5	0.00051	0.00026	0.00003	-	-	-
KELLERHALS	311.8	139.4	9.0	14.6	7.7	0.9	-	-	-	-	-	-
AMAFCA	1650.5	339.1	39.5	-	-	-	0.00987	0.00646	0.01126	-	-	-
M&O	-	-	65.6	-	-	1.9	-	-	-	-	-	5.7
AVERAGE	1122.1	416.3	31.7	9.5	5.3	1.0	0.00274	0.00197	0.00617	5.0	3.9	3.0
HEC-RAS	615.3	524.6	400.5	8.3	4.6	3.5	0.00787	0.00727	0.00693	9.6	5.2	4.0
BANKFULL	-	-	400.5	-	-	3.5	-	-	0.00693	-	-	4.0
EXPECTED BEHAVIOR	DEG	AGG	AGG	DEG	DEG	AGG	DEG	DEG	DEG	DEG	DEG	DEG

LOWER SAN JUAN CREEK REACH 3 CHANNEL GEOMETRY REALTIONS												
EQUATION / PARAMETER	CHANNEL WIDTH (FT)			FLOW DEPTH (FT)			SLOPE (FT/FT)			VELOCITY (FPS)		
	Q_{100}	Q_{10}	Q_2	Q_{100}	Q_{10}	Q_2	Q_{100}	Q_{10}	Q_2	Q_{100}	Q_{10}	Q_2
BRAY - 1	544.5	233.2	13.0	8.0	4.7	0.8	-	-	-	-	-	-
BRAY - 2	620.4	265.2	14.7	8.5	5.0	0.8	0.00037	0.00063	0.00390	5.6	4.5	2.1
HEY	-	-	-	7.1	3.8	0.5	0.00022	0.00052	0.00949	-	-	-
A&C / LACEY*	410.0	208.6	20.9	-	-	-	-	-	-	4.5	3.4	1.4
CHANG	3212.5	1319.7	59.5	-19.8	-9.0	-0.5	0.00051	0.00026	0.00003	-	-	-
KELLERHALS	311.8	139.4	9.0	14.6	7.7	0.9	-	-	-	-	-	-
AMAFCA	1990.4	360.8	43.0	-	-	-	0.00551	0.00492	0.00982	-	-	-
M&O	-	-	65.6	-	-	1.9	-	-	-	-	-	5.7
AVERAGE	1181.6	421.1	32.2	9.5	5.3	1.0	0.00165	0.00158	0.00581	5.0	3.9	3.0
HEC-RAS	697.1	532.9	427.8	9.2	4.6	3.4	0.00429	0.00548	0.00647	7.6	4.7	3.7
BANKFULL	-	-	427.8	-	-	3.4	-	-	0.00647	-	-	3.7
EXPECTED BEHAVIOR	DEG	AGG	AGG	DEG	DEG	AGG	DEG	DEG	DEG	DEG	DEG	DEG

LOWER SAN JUAN CREEK REACH 4 CHANNEL GEOMETRY REALTIONS												
EQUATION / PARAMETER	CHANNEL WIDTH (FT)			FLOW DEPTH (FT)			SLOPE (FT/FT)			VELOCITY (FPS)		
	Q_{100}	Q_{10}	Q_2	Q_{100}	Q_{10}	Q_2	Q_{100}	Q_{10}	Q_2	Q_{100}	Q_{10}	Q_2
BRAY - 1	544.5	233.2	13.0	8.0	4.7	0.8	-	-	-	-	-	-
BRAY - 2	620.4	265.2	14.7	8.5	5.0	0.8	0.00037	0.00063	0.00390	5.6	4.5	2.1
HEY	-	-	-	7.1	3.8	0.5	0.00022	0.00052	0.00949	-	-	-
A&C / LACEY*	410.0	208.6	20.9	-	-	-	-	-	-	4.5	3.4	1.4
CHANG	3094.0	1268.0	56.5	-19.2	-8.7	-0.5	0.00051	0.00026	0.00003	-	-	-
KELLERHALS	311.8	139.4	9.0	14.6	7.7	0.9	-	-	-	-	-	-
AMAFCA	409.8	283.4	34.8	-	-	-	0.00502	0.00531	0.01040	-	-	-
M&O	-	-	65.6	-	-	1.9	-	-	-	-	-	5.7
AVERAGE	898.4	399.6	30.6	9.5	5.3	1.0	0.00153	0.00168	0.00595	5.0	3.9	3.0
HEC-RAS	520.4	406.2	321.0	9.6	5.1	3.5	0.00541	0.00591	0.00762	8.9	5.3	4.2
BANKFULL	-	-	321.0	-	-	3.5	-	-	0.00762	-	-	4.7
EXPECTED BEHAVIOR	DEG	AGG	AGG	AGG	DEG	AGG	DEG	DEG	DEG	DEG	DEG	DEG

LOWER SAN JUAN CREEK REACH 5 CHANNEL GEOMETRY REALTIONS												
EQUATION / PARAMETER	CHANNEL WIDTH (FT)			FLOW DEPTH (FT)			SLOPE (FT/FT)			VELOCITY (FPS)		
	Q_{100}	Q_{10}	Q_2	Q_{100}	Q_{10}	Q_2	Q_{100}	Q_{10}	Q_2	Q_{100}	Q_{10}	Q_2
BRAY - 1	544.5	233.2	13.0	8.0	4.7	0.8	-	-	-	-	-	-
BRAY - 2	620.4	265.2	14.7	8.5	5.0	0.8	0.00037	0.00063	0.00390	5.6	4.5	2.1
HEY	-	-	-	7.1	3.8	0.5	0.00022	0.00052	0.00949	-	-	-
A&C / LACEY*	410.0	208.6	20.9	-	-	-	-	-	-	4.5	3.4	1.4
CHANG	3330.2	1371.1	62.4	-20.4	-9.3	-0.6	0.00051	0.00026	0.00003	-	-	-
KELLERHALS	311.8	139.4	9.0	14.6	7.7	0.9	-	-	-	-	-	-
AMAFCA	454.1	270.6	33.0	-	-	-	0.00637	0.00803	0.01421	-	-	-
M&O	-	-	65.6	-	-	1.9	-	-	-	-	-	5.7
AVERAGE	945.2	414.7	31.2	9.5	5.3	1.0	0.00187	0.00236	0.00691	5.0	3.9	3.0
HEC-RAS	641.9	392.5	312.3	9.4	4.7	3.4	0.00603	0.00830	0.00856	9.2	6.1	4.7
BANKFULL	-	-	312.3	-	-	3.4	-	-	0.00856	-	-	4.7
EXPECTED BEHAVIOR	DEG	DEG	AGG	DEG	DEG	AGG	DEG	DEG	DEG	DEG	DEG	DEG

LOWER SAN JUAN CREEK REACH 6 CHANNEL GEOMETRY REALTIONS												
EQUATION / PARAMETER	CHANNEL WIDTH (FT)			FLOW DEPTH (FT)			SLOPE (FT/FT)			VELOCITY (FPS)		
	Q_{100}	Q_{10}	Q_2	Q_{100}	Q_{10}	Q_2	Q_{100}	Q_{10}	Q_2	Q_{100}	Q_{10}	Q_2
BRAY - 1	544.5	233.2	13.0	8.0	4.7	0.8	-	-	-	-	-	-
BRAY - 2	620.4	265.2	14.7	8.5	5.0	0.8	0.00037	0.00063	0.00390	5.6	4.5	2.1
HEY	-	-	-	7.1	3.8	0.5	0.00022	0.00052	0.00949	-	-	-
A&C / LACEY*	410.0	208.6	20.9	-	-	-	-	-	-	4.5	3.4	1.4
CHANG	3231.0	1327.7	59.9	-19.9	-9.0	-0.5	0.00051	0.00026	0.00003	-	-	-
KELLERHALS	311.8	139.4	9.0	14.6	7.7	0.9	-	-	-	-	-	-
AMAFCA	277.9	210.2	27.0	-	-	-	0.00563	0.00643	0.01101	-	-	-
M&O	-	-	65.6	-	-	1.9	-	-	-	-	-	5.7
AVERAGE	899.2	397.4	30.0	9.5	5.3	1.0	0.00168	0.00196	0.00611	5.0	3.9	3.0
HEC-RAS	351.6	275.3	235.4	11.7	5.2	3.8	0.00602	0.00676	0.00668	11.3	6.6	4.9
BANKFULL	-	-	235.4	-	-	3.8	-	-	0.00668	-	-	4.9
EXPECTED BEHAVIOR	DEG	DEG	AGG	AGG	DEG	AGG	DEG	DEG	DEG	DEG	DEG	DEG

LOWER SAN JUAN CREEK REACH 7 CHANNEL GEOMETRY REALTIONS												
EQUATION / PARAMETER	CHANNEL WIDTH (FT)			FLOW DEPTH (FT)			SLOPE (FT/FT)			VELOCITY (FPS)		
	Q_{100}	Q_{10}	Q_2	Q_{100}	Q_{10}	Q_2	Q_{100}	Q_{10}	Q_2	Q_{100}	Q_{10}	Q_2
BRAY - 1	544.5	233.2	13.0	8.0	4.7	0.8	-	-	-	-	-	-
BRAY - 2	620.4	265.2	14.7	8.5	5.0	0.8	0.00037	0.00063	0.00390	5.6	4.5	2.1
HEY	-	-	-	7.1	3.8	0.5	0.00022	0.00052	0.00949	-	-	-
A&C / LACEY*	410.0	208.6	20.9	-	-	-	-	-	-	4.5	3.4	1.4
CHANG	3500.7	1445.7	66.7	-21.3	-9.7	-0.6	0.00051	0.00026	0.00003	-	-	-
KELLERHALS	311.8	139.4	9.0	14.6	7.7	0.9	-	-	-	-	-	-
AMAFCA	248.2	180.5	23.0	-	-	-	0.00621	0.00716	0.01614	-	-	-
M&O	-	-	65.6	-	-	1.9	-	-	-	-	-	5.7
AVERAGE	939.3	412.1	30.4	9.5	5.3	1.0	0.00183	0.00214	0.00739	5.0	3.9	3.0
HEC-RAS	310.1	261.4	218.3	12.0	6.1	4.0	0.00636	0.00773	0.01007	11.7	6.9	5.7
BANKFULL	-	-	218.3	-	-	4.0	-	-	0.01007	-	-	5.7
EXPECTED BEHAVIOR	DEG	DEG	AGG	AGG	AGG	AGG	DEG	DEG	DEG	DEG	DEG	DEG

LOWER SAN JUAN CREEK REACH 8 CHANNEL GEOMETRY REALTIONS												
EQUATION / PARAMETER	CHANNEL WIDTH (FT)			FLOW DEPTH (FT)			SLOPE (FT/FT)			VELOCITY (FPS)		
	Q_{100}	Q_{10}	Q_2	Q_{100}	Q_{10}	Q_2	Q_{100}	Q_{10}	Q_2	Q_{100}	Q_{10}	Q_2
BRAY - 1	544.5	233.2	13.0	8.0	4.7	0.8	-	-	-	-	-	-
BRAY - 2	620.4	265.2	14.7	8.5	5.0	0.8	0.00037	0.00063	0.00390	5.6	4.5	2.1
HEY	-	-	-	7.1	3.8	0.5	0.00022	0.00052	0.00949	-	-	-
A&C / LACEY*	410.0	208.6	20.9	-	-	-	-	-	-	4.5	3.4	1.4
CHANG	3024.7	1237.8	54.8	-18.8	-8.5	-0.5	0.00051	0.00026	0.00003	-	-	-
KELLERHALS	311.8	139.4	9.0	14.6	7.7	0.9	-	-	-	-	-	-
AMAFCA	221.6	157.9	17.7	-	-	-	0.00488	0.00547	0.00870	-	-	-
M&O	-	-	65.6	-	-	1.9	-	-	-	-	-	5.7
AVERAGE	855.5	373.7	28.0	9.5	5.3	1.0	0.00149	0.00172	0.00553	5.0	3.9	3.0
HEC-RAS	284.2	233.9	152.8	14.2	7.4	5.2	0.00503	0.00608	0.00507	11.3	6.8	5.4
BANKFULL	-	-	152.8	-	-	5.2	-	-	0.00507	-	-	5.4
EXPECTED BEHAVIOR	DEG	DEG	AGG	AGG	AGG	AGG	DEG	DEG	AGG	DEG	DEG	DEG

In general, the channel geometry analysis indicates that San Juan Creek will tend to trend toward a wider, more shallow, and flatter (lower slope) channel than the present channel geometry. However, except for the 100-year discharge, channel velocities indicate that most flows may lack the energy to cause channel change. The velocity data generally predict fill rather than the scour predicted by the depth and slope calculations.

- <u>Natural channel width</u>. The main channel of the San Juan Creek appears to be adjusted to the flow width greater than the present 100-year event.
- <u>Channel depth</u>. The predicted channel depths vary compared the flow depths computed by HEC-RAS modeling. Therefore, a combination of aggradation and degradation during most floods should be expected in the future.
- <u>Channel slope</u>. The predicted channel slope is flatter than the existing channel slope in all reaches. Therefore, long-term scour (degradation) should be expected.

- Channel velocity. In general, the predicted velocities are higher than the velocities computed by HEC-RAS modeling for the 100-year event. Therefore, sediment scour and long-term degradation is predicted by these equations. However, when compared to the results for width, depth, and slope, the predictions of fill for most reaches for lower discharges suggests the formation of a new channel geometry which has as yet largely not been formed.
- The new channel geometry according to these computations is likely to be wider, more shallow, and flatter, with higher velocities in the channel than under the current conditions.

The predicted channel geometry values were compared to the estimated bankfull geometry values described elsewhere in this chapter. The approximate recurrence interval of the bankfull discharge channel geometry computed using HEC-RAS modeling was estimated by plotting the average 2, 10, and 100-year channel geometry results versus probability and interpolating between data points. The data used from the channel geometry equations excluded consideration of cross sections at or near bridges as well as the channelized reaches. The reach-average data were compared to the median bankfull geometry data.

Methodology- Hydraulic data were obtained from the modified HEC-RAS model. These data were used to develop reach-averaged regression equations using the form and variables of the classic hydraulic geometry equations established in Leopold and Maddock (1953). The following three (3) equations were developed using the Microsoft Excel multiple regression statistical software package:

$$\mathbf{w \;\alpha\; aQ^{b}} \qquad \mathbf{d \;\alpha\; cQ^{f}} \qquad \mathbf{v \;\alpha\; kQ^{m}}$$

Where w = width; channel topwidth (ft.)
Q = discharge; channel discharge (cfs)
d = depth; hydraulic channel depth (ft.)
v = velocity, channel velocity (ft/s)
a, c, k = coefficients
b, f, m = exponents

The principles of continuity and dimensional analysis dictate that the regression equation coefficients relating change of depth, width, and velocity to change in discharge should equal one when multiplied together (i.e., $a \times c \times k = 1$). Similarly, the regression equation exponents also should have a sum of one $(b + f + m = 1)$. The expectation of continuity was met at the majority (96%) of river stations: of 444 stations in this study, only 17 did not meet the continuity criteria. Variations in continuity are likely caused by complicated multiple channel geometries and deficiencies in the HEC-RAS modeling.

The hydraulic geometry regression equations were used to evaluate expected channel change in several ways. First, exponents for velocity *(m),* depth *(f),* and width *(b)* in the study area were compared with the averages for ephemeral streams in the semiarid United States. In addition, the hydraulic geometry regression equations for each of the reaches were compared to identify anomalies that might indicate lateral or vertical instability. Second, the *m/f* ratio, an indication of the rate of sediment transport within the streams, was compared with the average for ephemeral streams in the semiarid United States. Leopold, Wolman, and Miller (1964) used the *m/f* ratio (change in velocity to change in depth with change in discharge) as an indicator of the rate of sediment transport. The greater the *m/f* ratio, the larger the amount of sediment transported with changes in discharge. Average at-a-station relationships for ephemeral streams in semiarid U.S. are $m = 0.34$ and $f = 0.36$. The average *m/f* ratio is thus 0.94.

Results-San Juan Creek - The hydraulic geometry equation exponents for width, depth, and velocity at each river station, are shown below. Wide variation between the hydraulic relationships of adjacent cross sections is evident. The exponent for hydraulic width varies widely around the average value for ephemeral streams. The increase in depth with increased discharge experienced by San Juan Creek tends to be above the average for ephemeral streams. Not surprisingly, the exponent for depth is consistently above average in the levee reach. Increases in velocity with increased discharge vary just as widely from average as do the increases in width and depth. The velocity increase tends to be slower than average in the more natural reaches and faster than average in the encroached and levee reaches. The hydraulic geometry equations emphasize the variability of San Juan Creek from station to station.

The large variability of the hydraulic geometry exponents makes identification of longitudinal trends difficult. Therefore, hydraulic geometry equations for each reach were calculated using the HEC-RAS model results from the river stations within the reach. Bridge cross sections were removed from the computations in order to reflect more accurately the average (non-constricted) conditions in the reach. *Table 7-4* lists the computed hydraulic geometry equation exponents for each of the eight (8) delineated reaches in the study area.

Table 7-4: Hydraulic Geometry Equations – San Juan Creek

Stream/ Reach	Width ($w=aQ^b$)		Depth ($d=cQ^f$)		Velocity ($w=kQ^m$)		a x c x k	b + f + m
	a	b	c	f	k	m		
San Juan Creek								
1	79.61	0.12	1.86	0.14	0.01	0.74	1.04	1.00
2	41.32	0.27	0.07	0.43	0.33	0.29	1.00	1.00
3	126.80	0.11	0.02	0.60	0.38	0.30	0.99	1.00
4	27.74	0.35	0.09	0.39	0.40	0.26	1.00	1.00
5	22.22	0.40	0.09	0.36	0.50	0.23	1.00	1.00
6	24.78	0.38	0.10	0.37	0.38	0.26	0.99	1.01
7	38.37	0.31	0.08	0.40	0.31	0.29	0.95	1.01
8	59.40	0.23	0.06	0.47	0.30	0.30	1.00	1.00
Entire	29.25	0.35	0.22	0.30	0.16	0.36	1.01	1.00

Comparison of Reaches to Arid West Streams. Leopold, Wolman, and Miller (1964) reported the following hydraulic geometry equation exponents for width:discharge (b), depth:discharge (f), and velocity:discharge (m):

$b=0.29$ $f=0.36$ $m=0.34$

Comparison to Previous Studies on San Juan Creek. The hydraulic geometry regression equation results provide some insight into the stability of the stream channels in the study area. A slower increase in depth and a faster increase in width indicate a channel configuration that is shallower than average and wider than average, a conclusion that is supported by the channel geometry equations described above. A faster increase in width as discharge increases might imply that the channel has poorly-consolidated banks, resulting in larger constraining lateral erosion while concentrating erosive work on the bed of the channel, as was hypothesized by Parker (1979). These factors, along with a faster increase in depth, might indicate that the channels are more incised than the average ephemeral wash.

7.6 Geomorphic Relationships - Engineering Methods Stability Assessment

7.6.1 Allowable Velocity

Allowable velocity criteria have long been used in channel design to estimate the velocity at which channel bed and bank sediments will begin to erode. A variety of allowable velocity data have been published by the US Army Corps of Engineers (1970, 1990, 1995) and the USDA Soil Conservation Service (1977), as well as by many other agencies.

Methodology- The following allowable velocity approaches were applied to the three (3) major streams in the study area:

- Fortier & Scobey Table
- BUREC/Mavis & Laushey Equation

- Neill Equation
- USACOE Permissible Velocity Tables

Fortier & Scobey Table. Fortier and Scobey (1926) published one (1) of the first tables of permissible velocity in 1926. Their data, based on records of seasoned stable canals, was later republished by a number of federal agencies and other organizations including the FHWA, ASCE, and Chow (MacBroom, 1981). The Fortier and Scobey data (*Table 7-5*) distinguish erosion hazards for clear water, silt-laden water, and water transporting sand and gravel (bedload). Their data presumably do not account for the stabilizing effect of bank vegetation. Further modifications to this method are described in Chow (1959) from Soviet researchers in 1936. These modifications include an adjustment to the permissible velocity based on depth. An additional modification was proposed by Lane (1955) for sinuous channels.

Table 7-5: Fortier & Scobey Table of Permissible Canal Velocities (ft/s)

Bank Material	Clear Water	Silt-Laden	Sand/Gravel Bedload
Sandy Loam	1.75	2.50	2.00
Firm Loam	2.50	3.50	2.25
Fine Gravel	2.50	5.00	3.75
Stiff Clay	3.75	5.00	3.00
Coarse Gravel	4.00	5.50	6.50
Cobbles	5.00	5.50	6.50

BUREC/Mavis & Laushey Equation. The BUREC (1974) recommends that permissible velocity be estimated using a modification of the Mavis and Laushey equation (Jurnikis, 1971), which was developed by bridge engineers in Great Britain (MacBroom, 1981). The BUREC equation is a function of grain size, and is most applicable to bed material.

$\mathbf{V_b = 0.64\ ^{D(4/9)}}$ for D < 6.0 mm
$\mathbf{V_b = 0.5\ D^{1/2}}$ for D > 6.0 mm

Where V_b = competent velocity (ft/sec)
D = particle diameter (mm)

Neill Equation. Neill (1975) developed equations that are a function of flow depth and grain size for permissible velocities on gravel and cobble bed streams, with a separate equation for cohesive soils.

$\mathbf{V_b = 3.15\ d^{(1/3)}\ D^{(2/3)}}$ (non-cohesive soils)
$\mathbf{V_b = 7.5\ d^{(1/6)}\ \tau_c\ ^{1/2}}$ (for cohesive soils)

Where V_b = competent velocity (ft/sec)
d = flow depth (ft) D = grain size (ft)
τ_c = critical shear stress (lb/ft^2)

USACOE Permissible Velocity. The Corps of Engineers (1970; 1995) has established suggested maximum velocities for design of non-scouring flood control channels of various bank materials, as shown in *Table 7-6*.

Table 7-6: Suggested Maximum Permissible Mean Channel Velocities (USACOE, 1995)

Channel Material	Mean Velocity (ft/sec)
Fine Sand (0.075 – 0.45 mm)	2.0
Coarse Sand (2 – 5 mm)	4.0
Fine Gravel (5 - 20 mm)	6.0
Grass-Lined Banks (< 5% Slope, Sandy Silt, Bermuda Grass)	8.0
Poor Rock (Sedimentary)	10.0
Good Rock (Igneous or Metamorphic)	20.0

The Corps of Engineers (1990) has also developed criteria relating flow depth and velocity to the beginning of movement of granular bed materials and erosion of cohesive bank materials, as summarized in *Table 7-7.*

Table 7-7: Corps of Engineers Erosive Velocity Data

Grain Size (mm)	Flow Depth (ft)	Velocity (ft/sec)
1 (sand)	5 10	2.5 4.0
10 (gravel)	5 10	4.5 5.5
100 (cobbles)	5 10	9.5 10.5

Results- In general, the internal alluvial banks of San Juan Creek are composed of sand, gravel and cobbles with different densities of bank and bed vegetation cover. *Table 7-8* shows the reach average velocity for all cross sections in the HEC-RAS for each reach.

The reach-average data show that the San Juan Creek is marginally erosive in the upper reaches and becomes more erosive, according to the permissible velocities shown in *Table 7-9*, in the finer-grained lower reaches. The most erosive conditions will occur at bridges and within the channelized reaches. Overbank velocities are generally below the erosive limit for gravels, but slightly higher than the erosive limit for sands. Since many of the overbank areas are composed of finer-grained materials, at least at the surface, erosion of the upper layers of the overbank areas is expected during a 100-year flood.

Table 7-8: San Juan Creek Reach Averaged Flood Velocities

Average Channel Velocity (fps)			
Reach	**100-Year**	**10-Year**	**2-Year**
1	10.4	6.4	4.7
2	9.6	5.2	4.0
3	7.6	4.7	3.7
4	8.9	5.3	4.2
5	9.2	6.1	4.7
6	11.3	6.6	4.9
7	11.7	6.9	5.7
8	11.3	6.8	5.4

The reach-average data for the 2-year flood show that San Juan Creek is erosive throughout all the reaches since the average velocities exceed the maximum allowable permissible of 4 fps. For the 2-year flood, the most erosion will occur at the few bridges and channelized reaches where velocities exceed the erosive thresholds. Since the main channel generally contains the 2-year flood at most cross sections, there will be limited flow and hence, erosion, in the overbanks. For those sections where overbank flow does occur, velocities are generally non-erosive.

Table 7-9: Allowable Velocity Results (fps)

100-Year				
Reach	**Fortier-Scobey**	**BUREC-Mavis-Laushey**	**Neill**	**USACOE**
1	2.0	1.4	0.6	4.0
2	2.0	1.4	0.6	4.0
3	2.0	1.4	0.6	4.0
4	2.0	1.4	0.6	4.0
5	2.0	1.4	0.6	4.0
6	2.0	1.4	0.6	4.0
7	2.0	1.4	0.6	4.0
8	2.0	1.4	0.7	4.0
10-Year				
Reach	**Fortier-Scobey**	**BUREC-Mavis-Laushey**	**Neill**	**USACOE**
1	2.0	1.4	0.5	4.0
2	2.0	1.4	0.5	4.0
3	2.0	1.4	0.5	4.0
4	2.0	1.4	0.5	4.0
5	2.0	1.4	0.5	4.0
6	2.0	1.4	0.5	4.0
7	2.0	1.4	0.5	4.0
8	2.0	1.4	0.5	4.0
20-Year				
Reach	**Fortier-Scobey**	**BUREC-Mavis-Laushey**	**Neill**	**USACOE**
1	2.0	1.4	0.4	4.0
2	2.0	1.4	0.4	4.0
3	2.0	1.4	0.4	4.0
4	2.0	1.4	0.4	4.0
5	2.0	1.4	0.4	4.0
6	2.0	1.4	0.4	4.0
7	2.0	1.4	0.4	4.0
8	2.0	1.4	0.5	4.0

The reach-averaged velocities estimated from the HEC-RAS models for the 2, 10, and 100-year events shown in *Table 7-8* were compared to the allowable velocities determined by the methodologies described above, as shown in *Table 7-9*. Erosion (E) is expected where the allowable velocities are exceeded by the predicted HEC-RAS reach-averaged velocities. Where the allowable velocities are not exceeded, the channel is expected to be stable (S).

Most of the allowable velocity methodologies used indicates that the materials in the bed and banks of the San Juan Creek are erodible. However, Neill's equation for cohesive soils predicts that the banks will be stable up to the 100-year event, even though the 100-year channel velocities approach or exceed the USACOE values of erodibility for igneous bedrock. Since cohesive soils are generally not present within the study area, the results of Neill's cohesive soil equation are not applicable for most of the reach. Comparison of HEC-RAS channel velocities with the USACOE and Fortier & Scobey erosive velocity thresholds indicate that the channel banks are probably erodible during flows that exceed the 2-year event.

Conclusions-San Juan Creek - Allowable velocity criteria provide general information on the likelihood of bank and channel erosion. However, accurate predictions of lateral stability based on allowable velocity criteria are difficult to achieve because of the effect of soil cohesiveness, vegetation, carbonate accumulations, and soil physics on erodibility. The range of allowable velocities indicated by the Neill equations illustrates the effect of cohesion on erodibility. Broadly interpreted, the allowable velocity data indicate that all of the channel banks in the study area will erode even in small floods if the banks are not cohesive, but will resist erosion if they are cohesive. Finally, the effects of bank vegetation (increase stability), stratified bank sediments (decrease stability), and other local variations (piping, bed scour, etc.) create additional uncertainty for the reliability of allowable velocity predictions.

7.6.2 Equilibrium Slope

Equilibrium slope is defined as the slope which causes the channel's sediment transport capacity to equal the incoming sediment supply (ADWR, 1985). If the slope is too steep, channel velocities will be high and net erosion will occur. If the slope is too flat, channel velocities will be low and net deposition will occur. The equilibrium slope is the slope that the undisturbed, natural channel will tend towards over the long term. While there are philosophical and practical problems with applying equilibrium slope concepts to ephemeral streams with variable channel geometry and high flash flood potential, or streams where the natural hydrology has been altered by urbanization or construction of dams, equilibrium slope equations provide a useful order-of-magnitude assessment of the likelihood of vertical channel adjustments.

7.6.3 Methodology

Reach-averaged data required for application of equilibrium slope equations to the study area were derived from the following sources:

- Hydraulic data - HEC-RAS modeling
- Hydrologic data - HEC-1 modeling and USGS gauge records
- Topographic data – Floodplain delineation studies

Most equilibrium slope equations are based on the mean annual flood, the "channel-forming," or "bankfull" discharge. On many alluvial streams, the mean annual flood and the channel-forming and bankfull discharges are nearly equivalent. However, on ephemeral streams where flow events are rare, the average annual discharge is often difficult to determine. To account for the discrepancies in what flow rate is appropriate for equilibrium slope analyses, and to assess the trend of expected slope adjustments during floods, the 2, 10, and 100-year peaks were used in the equilibrium slope equations to assess the expected slope adjustment over a range of discharges. The 2-year event approximates the mean annual flood calculated on a weighted probability basis. The 10-year event better approximates bankfull conditions in the study reach. The 100-year event represents possible channel responses during extreme flooding. The following equilibrium slope equations were applied to the study reach:

- Albuquerque Metropolitan Arroyo Flood Control Authority (AMAFCA) Equations
- BUREC Equation
- Bray Equation
- Henderson Equation
- Schoklitsch Equation
- Meyer-Peter Muller Equation
- Shield's Diagram Method
- Lane's Tractive Force Method

AMAFCA Equation. The AMAFCA (1994) equation for the maximum equilibrium slope is based on the sediment transport characteristics of the reach.

$$S_L = \left(\frac{a}{q_s}\right)^{\frac{10}{3(c-b)}} q^{\frac{2(2b+3c)}{3(c-b)}} \left(\frac{n}{1.49}\right)$$

Where S_L = channel slope (ft./ft.)
q_s = unit sediment transport (cfs/ft)
q = water discharge (cfs)
n = Manning's roughness
a, b, c = power function coefficients from sediment transport function

A simplified version of the AMAFCA Equation is written for wide, rectangular channels, similar to those in the study area, based on the assumptions that steep, wide, rectangular alluvial streams flow at or close to critical depth and that sediment supply is transport limited.

$$\mathbf{S_s = 18.28\ n^2\ F^{0.133}\ Fr^{2.133}\ Q_{dd}^{-0.133}}$$

Where S_s = Stable slope (ft/ft)
n = Manning's roughness value for the channel
F = Width/depth ratio of the channel
Fr = Froude number for the channel
Q_{dd} = Dominant discharge (cfs)

BUREC Equation. The BUREC published an equation for stable slope based on theoretical considerations of sediment transport (MacBroom, 1981).

$$\mathbf{S_L = (0.00021\ D_{50}\ W_{bf} / Q)^{0.75}}$$

Where S_L = Stable slope (ft/ft)
D_{50} = Bed sediment diameter (ft)
W_{bf} = Channel width (ft)
Q = Discharge (cfs)

Bray Equation. Bray's (1979) equation for equilibrium slope is based on regime analysis of perennial gravel bed streams in Alberta, Canada.

$$\mathbf{S_L = 0.965\ Q_2^{-0.344}\ D_{50}^{0.58}}$$

Where S_L = Equilibrium slope (ft/ft)
D_{50} = Mean bed sediment diameter (ft) Q_2= 2-year
discharge (cfs)

Henderson Equation. To generate an equation for the slope of stable channels, Henderson (1961) modified the Lane (1952) equations using a threshold theory of shear stress concept.

$$\mathbf{S_L = 0.44\ D_{90}^{1.15}\ Q^{-0.46}}$$

Where S_L = Stable slope (ft/ft)
D_{90} = Bed sediment diameter for which 90% is smaller (ft)
Q = Discharge (cfs)

The BUREC (Pemberton and Lara, 1984) published a manual for computing scour and channel degradation downstream of dams or other structures that interrupt the natural sediment supply to the downstream channel. The BUREC manual describes the following four approaches for estimating equilibrium slope: (1) Schoklitsch Equation, (2) Meyer-Peter Muller Equation, (3) Shield's Diagram Method, and (4) Lane's Tractive Force Method. The approaches are based on the assumption of zero sediment transport.

Schoklitsch Equation. The Schoklitsch (Shulits, 1935) equation is based on the concept of zero bedload transport.

$$\mathbf{S_L = K_s\ (D\ W_{bf}/Q)^{3/4}}$$

Where S_L = Stable slope (ft/ft)
K_s = 0.00174
W_{bf} = Bankfull width (ft)
D = Mean bed sediment diameter (mm)
Q = Dominant discharge (cfs)

Meyer-Peter, Muler Equation. The Meyer-Peter, Muller (1948) equation is based on the incipient motion theory, or the point of initiation of sediment transport.

$$\mathbf{S_L = K_{mpm}\ (Q/Q_{bf})\ (n_s/D_{90}\ ^{1/6})^{3/2}\ D\ /\ d}$$

Where S_L = Stable slope (ft/ft)
K_{mpm} = 0.19
Q/Q_{bf} = Ratio of total flow to flow over the channel
Q_{bf} = Dominant discharge (cfs)
n_s = Manning's 'n' for the stream bed
D_{90} = Bed sediment diameter for which 90% is smaller (mm)
D = Mean sediment diameter (mm)
d = Channel depth (ft)

Shields Diagram Method. The Shields diagram (1936) for determining the boundary condition for no sediment transport can be used to define an equation for stable slope.

$$\mathbf{R^* = U^*\ D\ /\ \nu}$$
$$\mathbf{U^* = (S_L\ R\ g)^{1/2}}$$
$$\mathbf{T^* = \tau_c\ /\ ((\gamma_s - \gamma_w)\ ^D)}$$

Where S_L = Stable slope (ft/ft)
R* = Boundary Reynold's number
U* = Shear velocity = (SL R g)^$^{0.5}$
D = Mean sediment diameter (mm)
ν = Kinematic velocity of water (ft/sec^2)
R = Hydraulic radius for wide channels (ft)
g = Gravitational constant = 32.2 ft/sec^2
T* = Dimensionless shear stress
τ_c = Critical shear stress (lb/ft^2)
γ_s = Specific weight of sediment (lb/ft^3)
γ_w = Specific weight of water (lb/ft^3)

Lane's Tractive Force Method. Lane's equation for stable slope uses critical tractive force relationships.

$$\mathbf{S_L = \tau_c\ /\ (\gamma_w\ d)}$$

Where S_L = Stable slope (ft/ft)

d = Mean flow depth (ft)
τ_c = Critical shear stress (lb/ft^2)
γ_w = Specific weight of water (lb/ft^3)

Table 7-10: Results of the Equilibrium Slope Analyses

Reach	AMAFCA (ft/ft)	BUREC (ft/ft)	Bray (ft/ft)	Henderson (ft/ft)	Schoklitsch (ft/ft)	MPM (ft/ft)	Shields (ft/ft)	Lanes (ft/ft)
1	0.0194	0.0011	0.0386	0.0224	0.0786	0.0004	0.0000	0.0163
2	0.0191	0.0013	0.0386	0.0224	0.0920	0.0005	0.0000	0.0208
3	0.0105	0.0014	0.0386	0.0224	0.1010	0.0005	0.0000	0.0189
4	0.0129	0.0011	0.0386	0.0224	0.0811	0.0005	0.0000	0.0180
5	0.0148	0.0013	0.0386	0.0224	0.0949	0.0004	0.0000	0.0185
6	0.0131	0.0008	0.0386	0.0224	0.0605	0.0003	0.0000	0.0148
7	0.0145	0.0008	0.0386	0.0224	0.0550	0.0003	0.0000	0.0145
8	0.0114	0.0007	0.0386	0.0224	0.0515	0.0003	0.0000	0.0122

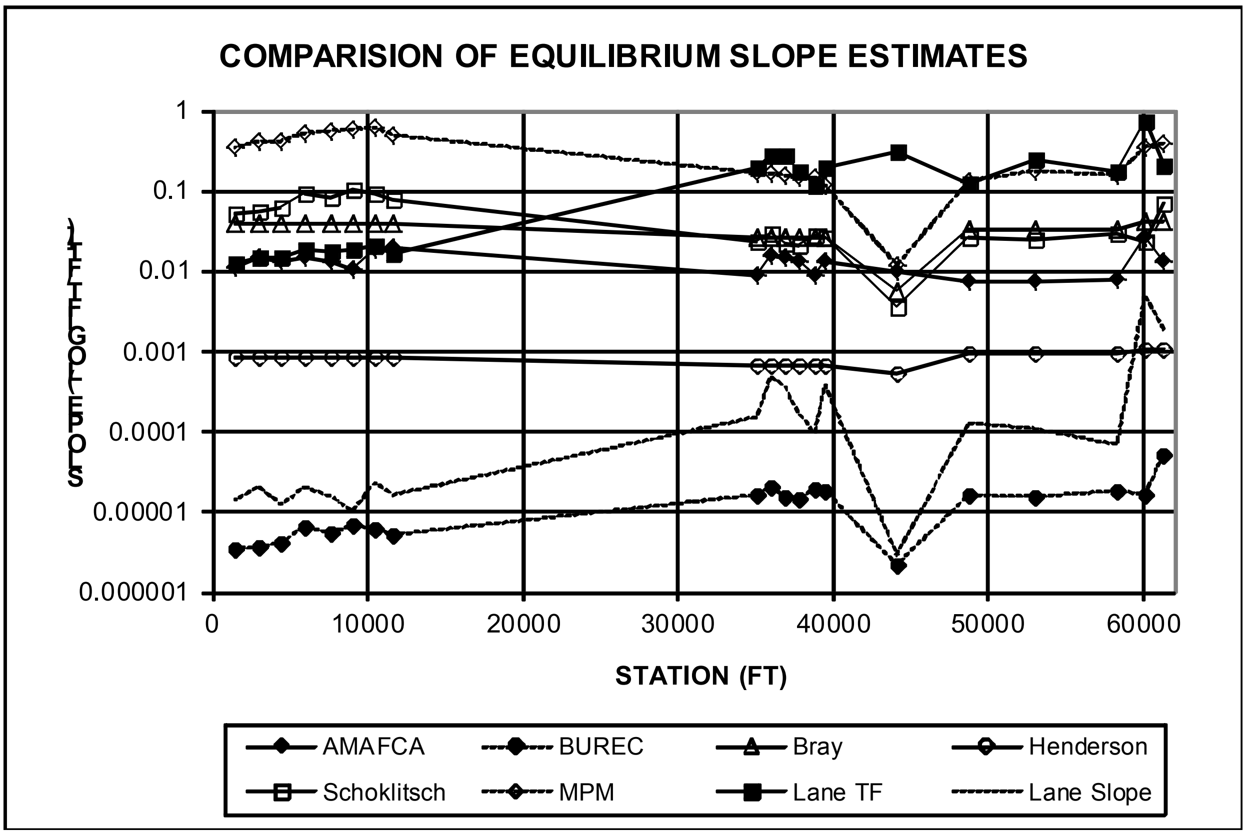

Figure 7-17: San Juan Creek Comparison of Equilibrium Slope Estimates

Reach-averaged equilibrium slope does not show a distinct trend. The variation in values is more than two orders of magnitude for the various methodologies. The parameters utilized in the development of the methodologies do not correspond well to the data measured in this project, which contributes to the widespread results. The results of the methodologies are included for completeness, although the values are not used for slope change estimates. The table above provides the reach-averaged equilibrium slopes while the graph illustrates the specific cross section calculated equilibrium slope.

Summary-San Juan Creek - The scour and deposition caused by the channel's adjustment to its equilibrium slope will be limited to a reach length sufficient for the channel to regain a sediment transport balance The middle reaches can expect to experience little change in slope or some aggradation for the periods dominated by small floods, with long-term degradation more likely to occur during periods dominated by large floods. The lower reaches are expected to experience long-term degradation, regardless of discharges that occur in the future. However, the extent of vertical adjustment will be limited by existing grade control structures within the channelized reaches. The actual magnitude of the expected bed elevation changes will be based in part on the potential for armoring, sediment supply, and the magnitude and frequency of the flows experienced in the future. The results of the equilibrium slope analysis are consistent with the analyses summarized earlier in this chapter in that they indicate that minimal channel change will occur during the small floods, and that more significant erosion will occur during the large floods.

7.6.4 Armoring

When the channel sediment transport capacity exceeds the upstream sediment supply, the balance of the sediment load may be eroded from the channel bed, causing the channel to degrade. Because fine sediments can be transported at more frequent lower discharges and velocities than coarse sediments, which may require large floods to be moved, fine sediment tends to be preferentially removed from the channel bed. Selective removal of fine sediments causes channel bed material to become progressively coarser over time, as long as the upstream sediment supply is limited. If this process continues over a long period, it ultimately creates a surficial layer of coarse channel sediments, called an armor layer, that the stream is incapable of transporting (Yang, 1996).

Methodology - The BUREC (Pemberton and Lara, 1984) recommends the following methodologies for estimating the minimum sediment size and depth of scour required to form an armor layer for a given flow rate:

- Meyer-Peter, Muller Bedload Transport Function
- Competent Bottom Velocity
- Shields Diagram
- Yang Incipient Motion

Meyer-Peter, Muller Bedload Transport Function*.* The Meyer-Peter, Muller (1948) bedload sediment transport function for the beginning of transport of individual grain sizes can be used to estimate the non-transportable sediment size.

$$\mathbf{D_c = d\ S\ /\ (K_{mpm}\ (n/D_{90}{}^{(1/6)})^{3/2})}$$

Where D_c = Non-transportable sediment diameter (mm)
d = Average flow depth (ft)
S = Energy slope (ft/ft)
K_{mpm} = 0.19
n = Manning's 'n' for the stream bed
D_{90} = Particle size for which 90% of the bed material is finer (mm)

Competent Bottom Velocity*.* This methodology is based on the work of Mavis and Lushey (1948), who developed an equation for the beginning of sediment movement on a stream bed.

$$\mathbf{D_c = 1.88\ V_m^{\,2}}$$

Where D_c = Armor size (mm)
V_m = Average channel velocity (ft/s)

Shields Diagram*.* The Shields (1936) diagram is a standard method used to define the initiation of motion for various channel bed sediment sizes. The method uses an iterative process to compute dimensionless shear stress (T*) and the armor diagram from the Shields diagram.

$$\mathbf{T^* = \tau_c / ((\gamma_s - \gamma_w)\ D_c)}$$

Where T* = Dimensionless shear stress
D_c = Armor size (mm)
τ_c = Critical shear stress (lb/ft^2)
γ_s = Specific weight of water = 62.4 lb/ft^3
γ_w = Specific weight of sediment = 165 lb/ft^3

Note that for gravel sediment sizes and turbulence levels typical in natural streams:

T* = 0.05 For sediment sizes greater than 1 mm and Boundary Reynold's Number (R*) > 500

Yang Incipient Motion*.* Yang (1973) developed a relationship between dimensionless critical velocity (V_{cr}/w, where w = fall velocity, ft/s) and shear velocity Reynold's number R* at incipient motion. Under natural stream conditions for sediment sizes greater than 2 mm, Yang's equation can be written as follows:

$$\mathbf{D_c = 0.00659\ V_{cr}^{\ 2}} \qquad \text{(For D > 2 mm)}$$

Where D_c = Armor size (ft)
V_{cr} = Critical average velocity at incipient motion (ft/s)

Depth to Armor Equation*.* Once the size of material (Dc) that will form an armor layer is estimated from one (1) or more of the equations listed above, the depth of scour required to form a stable armor layer can be estimated from the sediment distribution of the channel bed material. The equation for the depth to armor is the following:

$$\mathbf{Y_d = y_a\ (1/\Delta p - 1)}$$

Where Y_d = Depth from original streambed to the bottom of the armor layer (ft)
y_a = Thickness of the armor layer (ft)
Δp = Decimal percentage of the bed material larger than the armor size

Results-San Juan Creek - The results of the application of the BUREC armoring methodologies to the study area are summarized in *Table 7-11*. Channel sediment size distribution data for the study reach were compared with the critical armoring sediment diameter. If the computed depth to armor is excessive, and no evidence of armoring was observed in nearby reaches during the field work, it was assumed that formation of an armor layer was unlikely. As shown in *Table 7-11*, the bed of the San Juan Creek will armoring during most flood events and it does not require much scour depth to form the armor layer which is consistent with the observations of the streambed which indicates armor layers apparent in many portions of the streambed. The results of the armoring analysis indicates that the bed material is large enough to form an armor layer in some reaches at the 10 and 2-year peak discharge rates in the Upper and Middle Reaches. However, in the Lower Reach the actual depth of scour and duration of flow during a 2-year flood is insufficient to cause an armor layer to fully develop. Field evidence suggests that the armor layers may form locally in cobble riffles in the Upper Reach. One consequence of the formation of armor locally is an increase of lateral erosion of the banks along these riffles as the flood water searches to satisfy additional sediment load prevented from entrainment by the local armor layer.

Table 7-11: Armor Depth Results

100-Year					
Reach	Critical Armor Diameter (mm)				Depth to Armor (ft)
	MPM	CBV	Yang	Average	
61295	66.8	33.6	35.9	45.4	0.4
60149	170.8	159.0	169.9	166.6	1.6
58274	93.1	72.2	77.1	80.8	0.8
53099	81.4	88.2	94.3	87.9	0.9
48824	74.5	76.9	82.2	77.9	0.8
44098	132.7	74.4	79.5	95.5	0.9
39524	121.5	88.6	94.7	101.6	1.0
38848	45.0	63.1	67.4	58.5	0.6
37873	53.7	106.8	114.1	91.6	0.9
36882	85.7	117.5	125.5	109.6	1.1
35974	103.6	90.1	96.3	96.7	1.0
35121	45.1	74.9	80.1	66.7	0.7
33353	145.6	107.2	114.5	122.4	1.2
31022	134.8	75.1	80.2	96.7	1.0
28989	227.9	89.0	95.1	137.3	1.4
25776	150.4	87.3	93.3	110.3	1.1
22946	114.6	76.9	82.2	91.2	0.9
19502	247.4	120.0	128.2	165.2	1.6
10-Year					
Reach	Critical Armor Diameter (mm)				Depth to Armor (ft)
	MPM	CBV	Yang	Average	
61295	41.0	34.6	36.9	37.5	0.4
60149	115.1	60.2	64.3	79.9	0.8
58274	57.0	42.8	45.8	48.5	0.5
53099	37.3	31.1	33.3	33.9	0.3
48824	45.9	40.5	43.3	43.2	0.4
44098	24.3	38.1	40.7	34.4	0.3
39524	32.8	32.7	35.0	33.5	0.3
38848	33.5	37.8	40.4	37.2	0.4
37873	26.5	39.8	42.5	36.3	0.4
36882	34.9	57.3	61.2	51.1	0.5
35974	40.5	39.0	41.7	40.4	0.4
35121	26.8	27.7	29.6	28.0	0.3
33353	69.7	33.5	35.8	46.3	0.5
31022	96.6	45.3	48.4	63.4	0.6
28989	109.1	47.7	50.9	69.2	0.7
25776	74.8	37.4	40.0	50.7	0.5
22946	68.6	36.1	38.5	47.7	0.5
19502	157.3	53.4	57.1	89.3	0.9

Reach	2-Year				
	Critical Armor Diameter (mm)				Depth to Armor (ft)
	MPM	CBV	Yang	Average	
61295	16.7	7.6	8.2	10.8	0.1
60149	52.3	15.9	17.0	28.4	0.3
58274	24.7	18.6	19.8	21.0	0.2
53099	14.7	8.2	8.7	10.5	0.1
48824	21.2	11.2	12.0	14.8	0.1
44098	13.2	15.0	16.1	14.8	0.1
39524	12.2	11.0	11.7	11.7	0.1
38848	14.2	14.6	15.6	14.8	0.1
37873	11.1	12.0	12.8	11.9	0.1
36882	11.9	10.7	11.5	11.4	0.1
35974	17.5	11.1	11.9	13.5	0.1
35121	14.6	9.4	10.0	11.3	0.1
33353	27.3	9.8	10.5	15.9	0.2
31022	72.8	13.6	14.5	33.6	0.3
28989	42.4	15.1	16.2	24.6	0.2
25776	32.3	10.7	11.4	18.1	0.2
22946	30.0	9.1	9.8	16.3	0.2
19502	75.6	21.8	23.3	40.3	0.4

7.7 Chiquita Canyon Geomorphic Characteristics

7.7.1 Physical Setting

Chiquita Canyon is a relatively steep stream that oscillates back and forth between reaches that are characterized by deep incision with loss of access to its floodplain, to reaches where a relatively small main channel has access to a wide, shallow floodplain. The flow regime also alternates between subcritical and supercritical flow. The bed and bank are generally comprised of sandy soils. Some areas of moderately cohesive soils are present, as evidenced by near-vertical headcut formations of between 1 and 6 feet in height. A site visit was conducted in February 2011. Numerous photographs and descriptions of channel geomorphology were collected. This documentation is provided within the Floodplain Hydraulics/Sediment Technical Appendix.

7.7.2 Longitudinal Profile

Chiquita Canyon is characterized by a relatively steep profile with an average slope within the project limits of approximately 1.9%. A profile of the stream is shown below in *Figure 7-18*.

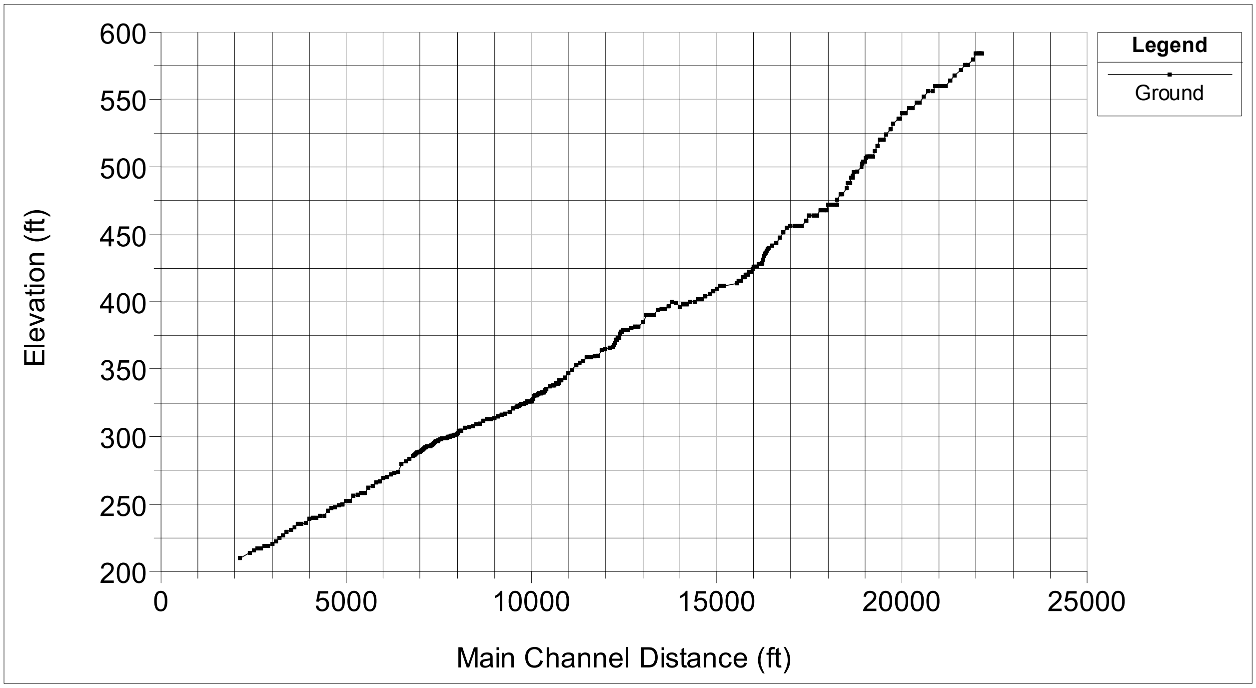

Figure 7-18 Chiquita Canyon – Profile of Existing Stream

As can be seen from the profile plot, the upper one-third of the stream is generally steeper than the lower two-thirds. The channel is marked by significant channel headcut formations, with headcuts often separating portions of incised channel downstream of the headcut and shallow channels with access to a wide floodplain upstream of the headcut. The headcuts are active and can be expected to continue with or without the proposed development activities. As the headcut process continues, additional bank failure and subsequent supply of stream channel sediment will continue.

7.7.3 Allowable Velocity

Allowable velocity criteria are discussed in Section 7.6. For this sand-bed stream, estimates of allowable velocity for the various methods presented in *Section 7.6* range between under 1 and 4 fps. *Table 7-12* presents reach-averaged, average channel velocities for the 2, 5, 10, 25, 50, and 100-yr storm events.

Table 7-12: Average Channel Velocity – Chiquita

Reach #	2-yr	5-yr	10-yr	25-yr	50-yr	100-yr
1	3.1	4.4	5.8	6.7	7.1	7.5
2	2.7	3.8	5	5.5	5.7	5.8
3	3.8	5.2	7.1	8	8.3	8.6
4	3.2	4.4	5.9	6.8	7.2	7.4
5	3	4.1	5.7	6.5	6.9	7.1
6	3.6	4.9	6.3	6.9	7.2	7.3
7	2.4	3.2	4.6	5.3	5.6	5.8
8	4	5.5	7.4	8.3	8.6	8.8
9	2.6	3.6	5.1	5.9	6.2	6.5
10	1.1	1.6	2.3	2.8	3	3.1
11	1.8	2.6	3.7	4.2	4.5	4.6
12	2.8	3.9	5.2	6.1	6.4	6.6
13	2.7	3.7	5	5.7	6	6.1

As demonstrated in *Table 7-12*, Chiquita Canyon is considered moderately erosive for the 2-year event. Average channel velocities significantly exceed allowable velocities for storms of higher magnitude. The data also illustrates that the upper portions of the stream trend toward higher velocities than the lower reaches.

7.7.4 Equilibrium Slope

Equilibrium slope analysis methodologies are discussed in *Section 7.6.2*. Equilibrium slope was computed for all reaches using the range of empirical equations. Detailed results are provided in the Floodplain Hydraulics/Sediment Technical Appendix. Based on these calculations, the AMAFCA equation was the only method that produced results within an order of magnitude of existing conditions. AMAFCA results are therefore used to aid in interpreting channel stability trends. The AMAFCA equation is based on sand-bed channels in Arizona and is the most representative of project conditions. *Figure 7-19* shows the comparison between existing Chiquita Creek channel gradient and the stable channel gradient computed by the various methods.

Table 7-13: Chiquita Canyon Equilibrium Slope Estimates

Reach	AMAFCA	BUREC	Henderson	Schoklitsch	MPM	Lanes	Existing Topo
	(ft/ft)	(ft/ft)	(ft/ft)	(ft/ft)	(ft/ft)	(ft/ft)	(ft/ft)
1	0.0097	0.0000	0.0001	0.0006	0.0006	0.0004	0.02626
2	0.0028	0.0000	0.0001	0.0016	0.0010	0.0005	0.00842
3	0.0030	0.0000	0.0001	0.0004	0.0005	0.0003	0.02962
4	0.0240	0.0000	0.0001	0.0004	0.0008	0.0002	0.02445
5	0.0158	0.0000	0.0001	0.0008	0.0010	0.0005	0.02863
6	0.0044	0.0000	0.0001	0.0004	0.0003	0.0002	0.01670
7	0.0013	0.0000	0.0001	0.0008	0.0005	0.0003	0.01275
8	0.0158	0.0000	0.0001	0.0003	0.0007	0.0002	0.01917
9	0.0090	0.0000	0.0001	0.0004	0.0010	0.0002	0.01343
10	0.0198	0.0000	0.0001	0.0015	0.0027	0.0005	0.01257
11	0.0086	0.0000	0.0001	0.0009	0.0021	0.0004	0.02016
12	0.0076	0.0000	0.0001	0.0005	0.0006	0.0002	0.01515
13	0.0578	0.0000	0.0001	0.0004	0.0015	0.0005	0.01606

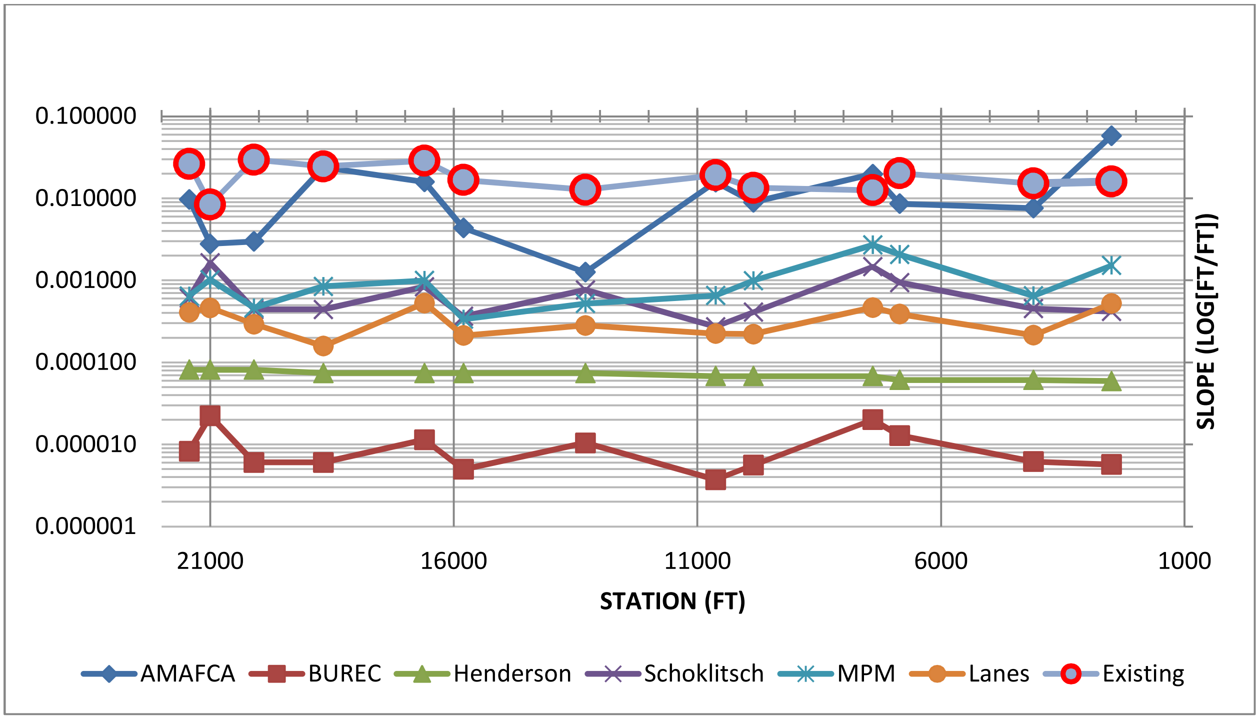

Figure 7-19 - Cañada Chiquita Comparison of Equilibrium Slope Estimates

The equilibrium slope is generally flatter than the existing slope. This suggests that there may be a tendency for the channel to degrade over time to achieve the equilibrium slope.

7.8 Cañada Gobernadora Geomorphic Characteristics

7.8.1 Physical Setting

Cañada Gobernadora is a relatively steep stream that oscillates back and forth between reaches that are characterized by deep incision with loss of access to its floodplain, to reaches where a relatively small main channel has access to a wide, shallow floodplain. The flow regime also alternates between subcritical and supercritical flow. However, Gobernadora has longer reaches of a consistent channel type and flow regime than does Chiquita Canyon. Gobernadora is susceptible to severe erosive events as evidenced by the December 2010 storm event. The bed and bank are generally comprised of sandy soils. Some areas of moderately cohesive soils are present, as evidenced by near-vertical headcut formations. A site visit was conducted in February 2011. Numerous photographs and descriptions of channel geomorphology were collected. This documentation is provided within the Floodplain Hydraulics/Sediment Technical Appendix.

7.8.2 Longitudinal Profile

Cañada Gobernadora is characterized by a relatively steep profile with an average slope within the project limits of approximately 1.2%. A profile of the stream is shown below in *Figure 7-20*.

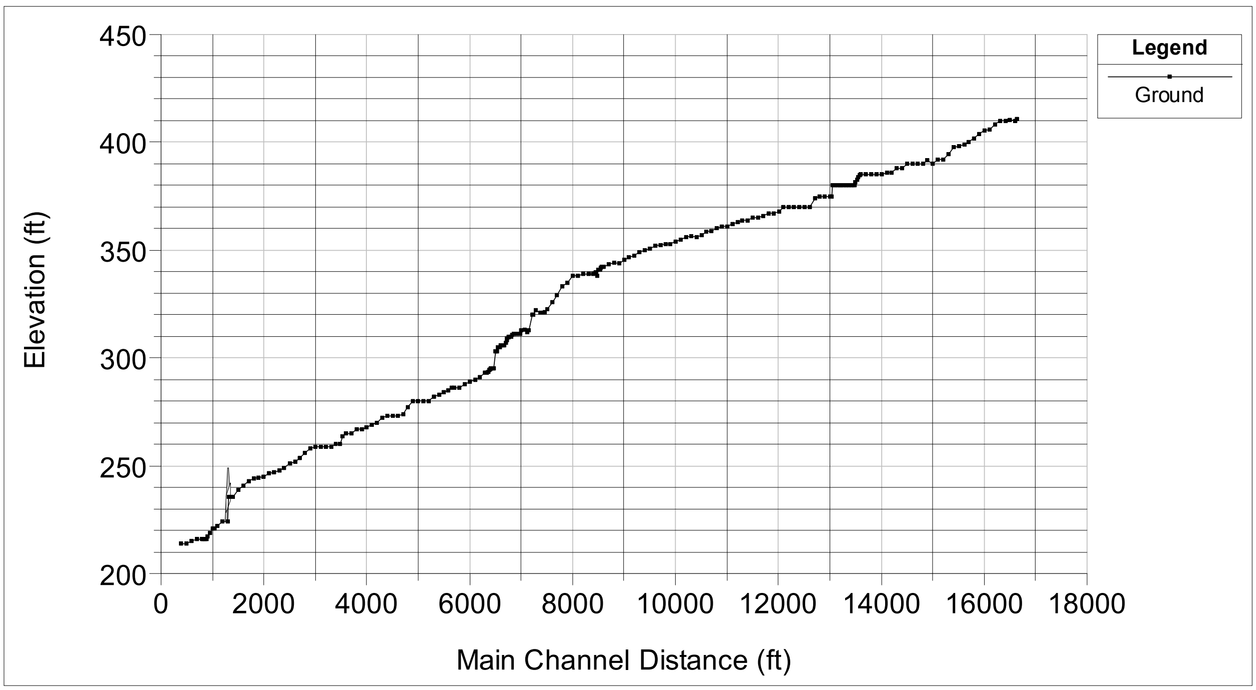

Figure 7-20 - Cañada Gobernadora – Profile Existing Streambed

The channel is marked by significant channel headcut formations, with headcuts often separating portions of incised channel downstream of the headcut and shallow channels with access to a wide floodplain upstream of the headcut. The headcuts are active and can be expected to continue with or without the proposed development activities. As the headcut process continues, additional bank failure and subsequent supply of stream channel sediment will continue.

7.8.3 Allowable Velocity

Allowable velocity criteria are discussed in *Section 7.6*. For this sand-bed stream, estimates of allowable velocity for the various methods presented in *Section 7.6* range between under 1 and 4 fps. *Table 7-14* presents reach-averaged, average channel velocities for the 2, 5, 10, 25, 50, and 100-yr storm events.

Table 7-14: Average Channel Velocity – Gobernadora

Reach #	2-yr	5-yr	10-yr	25-yr	50-yr	100-yr
1	3.30	4.40	5.70	6.40	6.60	6.90
2	3.00	3.70	4.90	5.50	5.80	6.00
3	2.30	2.90	3.80	4.40	4.70	4.80
4	2.50	2.70	3.20	3.60	3.80	4.00
5	1.40	1.70	2.20	2.60	2.70	2.90
6	1.10	1.60	2.10	2.30	2.40	2.50
7	5.00	5.90	7.10	7.70	8.00	8.20
8	3.90	4.90	6.10	6.80	7.10	7.30
9	4.60	5.90	7.40	8.30	8.80	9.00
10	2.00	2.70	3.10	3.40	3.60	3.70
11	3.10	3.90	5.00	5.60	6.00	6.20

As demonstrated in *Table 7-14,* Cañada Gobernadora is considered moderately erosive for the 2-year event. Average channel velocities significantly exceed allowable velocities for storms of higher magnitude for most reaches. The data also illustrates that reaches 5 and 6 maintain relatively low velocities for even the larger magnitude storm events.

7.8.4 Equilibrium Slope

Equilibrium slope analysis methodologies are discussed in *Section 7.6.2*. Equilibrium slope was computed for all reaches using the range of empirical equations. Detailed results are provided in the Floodplain Hydraulics/Sediment Technical Appendix. Based on these calculations, the AMAFCA equation was the only method that produced results within an order of magnitude of existing conditions. AMAFCA results are therefore used to aid in interpreting channel stability trends. The AMAFCA equation is based on sand-bed channels in Arizona and is the most representative of project conditions. *Figure 7-21* shows the comparison between existing Cañada Gobernadora channel gradient and the stable channel gradient computed by the various methods.

Table 7-15: Cañada Gobernadora Equilibrium Slope Estimates

Reach	AMAFCA	BUREC	Henderson	Schoklitsch	MPM	Lanes	Existing Topo
	(ft/ft)	(ft/ft)	(ft/ft)	(ft/ft)	(ft/ft)	(ft/ft)	(ft/ft)
1	0.009	0.000004	0.000040	0.0003	0.0006	0.0002	0.01222
2	0.0040	0.000005	0.000040	0.0003	0.0006	0.0002	0.00576
3	0.0063	0.000012	0.000040	0.0009	0.0007	0.0003	0.01026
4	0.0213	0.000010	0.000040	0.0007	0.0003	0.0002	0.00667
5	0.0046	0.000015	0.000040	0.0011	0.0017	0.0003	0.00770
6	0.0033	0.000017	0.000040	0.0013	0.0014	0.0003	0.00957
7	0.0047	0.000003	0.000040	0.0002	0.0002	0.0001	0.02727
8	0.0058	0.000003	0.000039	0.0002	0.0004	0.0001	0.01182
9	0.0114	0.000002	0.000039	0.0002	0.0003	0.0001	0.01001
10	0.0093	0.000012	0.000039	0.0009	0.0009	0.0003	0.01142
11	0.0041	0.000003	0.000039	0.0002	0.0003	0.0001	0.02240

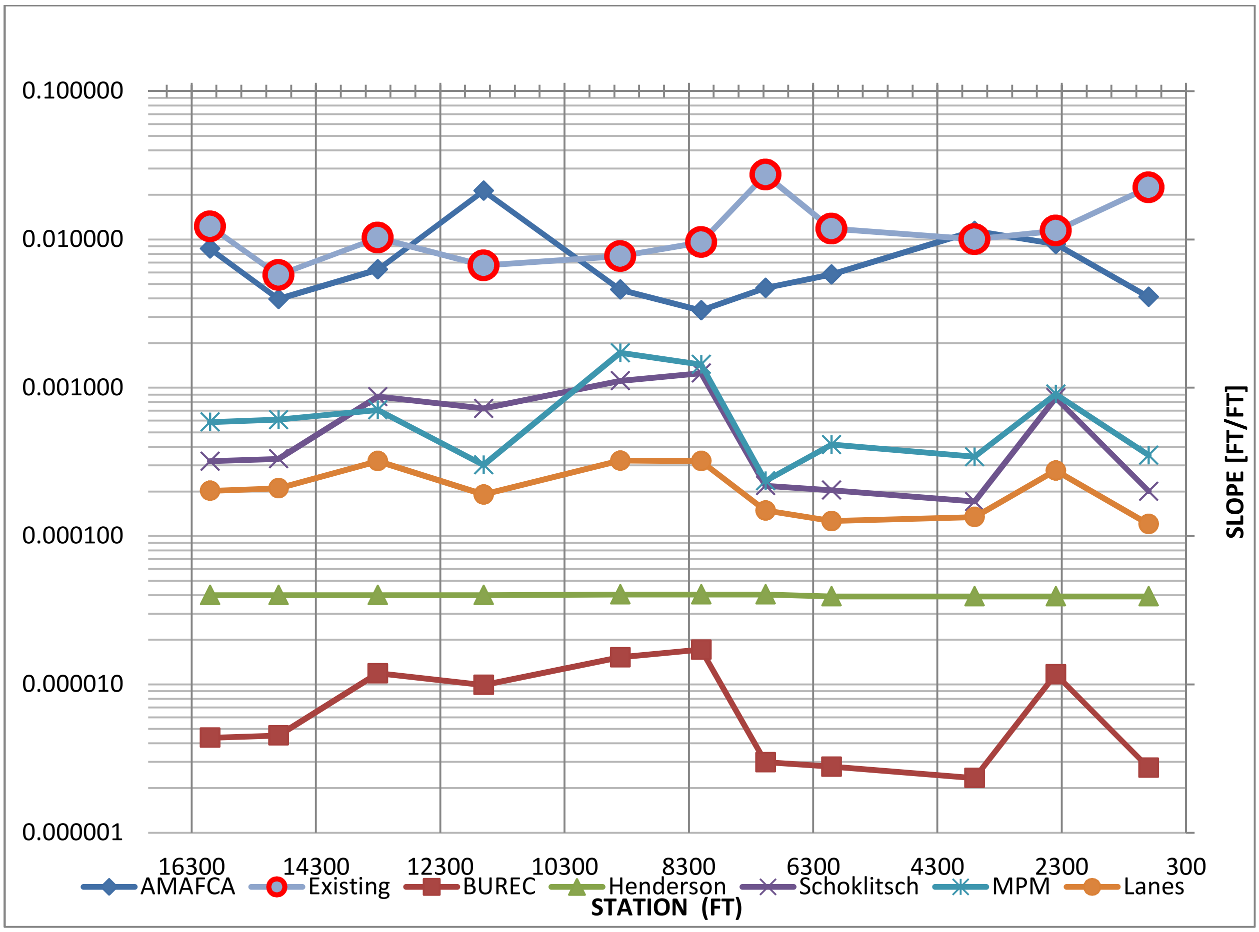

Figure 7-21: Cañada Gobernadora Comparison of Equilibrium Slope Estimates

The equilibrium slope is generally flatter than the existing slope. This suggests that there may be a tendency for the channel to degrade over time to achieve the equilibrium slope.